ACS Catalysis

Research Article

pubs.acs.org/acscatalysis

Computational Kinetic Discrimination of Ethylene Polymerization Mechanisms for the Phillips (Cr/SiO_2) Catalyst

Anthony Fong,[†] Ye Yuan,[†] Sam L. Ivry,[†] Susannah L. Scott,*[,†,‡] and Baron Peters*[,†,‡]

[†]Department of Chemical Engineering, [‡]Department of Chemistry & Biochemistry, University of California, Santa Barbara, Santa Barbara, California 93106-5080, United States

Supporting Information

ABSTRACT: The mechanism of ethylene polymerization by the widely used Phillips catalyst remains controversial. In this work, we compare initiation, propagation, and termination pathways computationally using small chromasiloxane cluster models for several previously proposed and new mechanisms. Where possible, we consider complete catalytic cycles and compare predicted kinetics, active site abundances, and polymer molecular weights to known properties of the Phillips catalyst. Prohibitively high activation barriers for propagation rule out previously proposed chromacycle ring expansion and Green−Rooney (alternating alkylidene/chromacycle) mechanisms. A new oxachromacycle ring expansion mechanism has a plausible propagation barrier, but initiation is prohibitively slow. On sites with adjacent bridging hydroxyls, either ≡Si(OH)Cr^{II}-alkyl or ≡Si(OH)Cr^{III}-alkyl, initiated by proton transfer from ethylene, chain growth by a Cossee−Arlman-type mechanism is fast. However, the initiation step is uphill and extremely slow, so essentially all sites remain trapped in a dormant state. In addition, these sites make only oligomers because when all pathways are considered, termination is faster than propagation. A monoalkylchromium(III) site without an adjacent proton, $(\equiv SiO)_2$Cr-alkyl, is viable as an active site for polymerization, although its precise origin remains unknown.

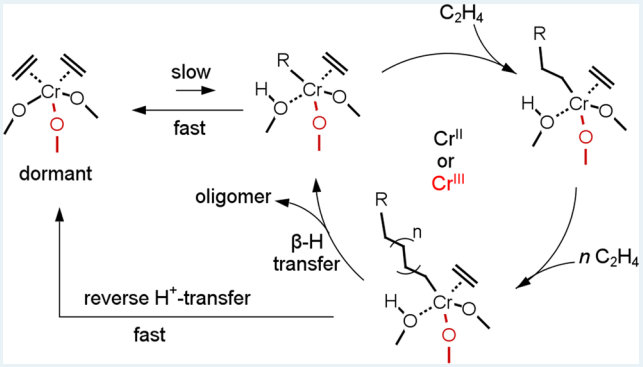

KEYWORDS: *Phillips catalyst, chromium, ethylene polymerization, density functional theory, initiation, chain termination*

1. INTRODUCTION

The Phillips catalyst (Cr/SiO_2), discovered serendipitously in 1951, is still used today in the annual production of nearly half of the world's supply of high-density polyethylene.[1] Phillips catalysts produce polyethylene with a weight-averaged molecular weight of 10^4−10^6 g/mol; a dispersity, $Đ$, of 4−100; and a steady-state polymerization rate of $(2–5) \times 10^3$ C_2H_4 s^{-1} Cr^{-1} at 373 K and 40 atm C_2H_4.[1,2] The polyethylene properties can be adjusted for pipe extrusion, film blowing, or other applications by modifying the catalyst. For example, increasing the catalyst calcination temperature usually lowers the average polymer molecular weight (and also enhances the activity).[3] The presence and amount of additional catalyst components (such as alkylaluminum reagents) can change the polymer density.[1,4] Incorporating titanium into the silica support causes chain transfer to accelerate and the molecular weight distribution, which determines toughness and creep resistance, to broaden.[1,5,6] Although numerous other methods for tailoring specific polymer attributes are known, there is little molecular-level understanding of how they work or even any consensus on the precise nature of the minority Cr active sites.

The mystery of how the inorganic precursor sites of the Phillips catalyst (CrO_x/SiO_2) spontaneously initiate polymerization has resisted sustained investigation by many research groups lasting several decades. Unlike other catalysts for α-olefin polymerization, the silica-supported chromate ester sites that are present in the precatalyst do not require an external source of alkyl or hydride groups to create the first polymer chains (Figure 1). The activated sites arise spontaneously during a pronounced induction period. In the most widely accepted mechanistic model, ethylene inserts into these initiating $(\equiv SiO)_2$Cr−H or $(\equiv SiO)_2$Cr−C bonds (Figure 2), and these alkylchromium(III) sites polymerize ethylene by repeated insertion of monomer (i.e., the Cossee−Arlman mechanism).[7] The growing polymer chain is eventually

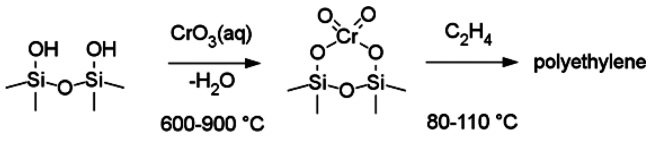

Figure 1. CrO_3 on amorphous silica forms grafted chromate esters, whose exposure to ethylene at ~100 °C results in spontaneous active site formation during a pronounced induction period, and subsequent polymer growth.[1,9]

Received: January 5, 2015
Revised: April 6, 2015
Published: April 9, 2015

DOI: 10.1021/acscatal.5b00016
ACS Catal. 2015, 5, 3360−3374

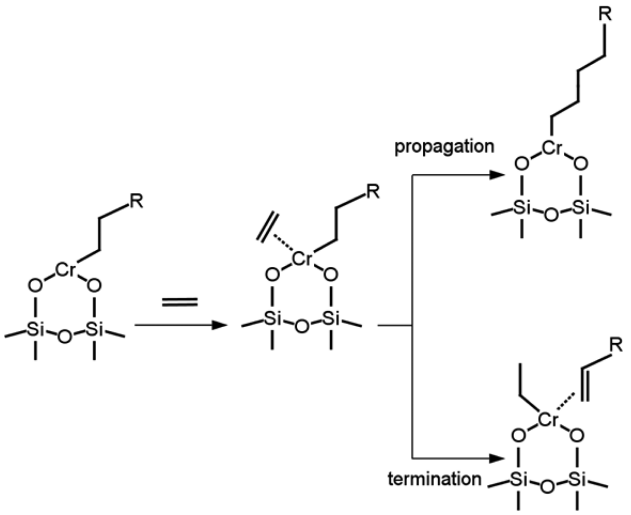

Figure 2. Proposed Cossee–Arlman mechanism[1,7] for Phillips polymerization by minority alkylchromium(III) sites formed in situ under reaction conditions. R is either H or an alkyl group.

expelled through β-H elimination or β-H transfer to an incoming ethylene molecule, and newly formed hydrido- or ethylchromium(III) sites continue the polymerization process. This mechanism is well-established for Ziegler–Natta catalysts, although those catalysts either possess pre-existing alkyl ligands or acquire them from alkylating agents (cocatalysts).[8]

For the Phillips catalyst, the Cossee–Arlman propagation mechanism requires that the initiating alkyl ligand (most likely with an odd number of H atoms) be formed from ethylene alone, with its even number of H atoms. This dilemma is known as the "missing hydrogen" problem.[1,7,10] In principle, the silica support could supply an additional proton from one of its surface hydroxyl groups. However, calcining the support to *remove* most of these hydroxyl groups is necessary to obtain an active catalyst, and higher calcination temperatures (up to 900 °C) actually cause the polymerization activity to increase further.[3] Isotopic labeling experiments[11] as well as first-principles calculations[12,13] are consistent with chain propagation by a Cossee–Arlman mechanism once the alkyl group is installed, although the evidence presented to-date consists largely of analogies to Ziegler–Natta catalysts[7] or the ruling out of other possible mechanisms.[11,13,14] There is still no accepted mechanism that explains the initial alkyl ligand generation.

Several alternative mechanisms that circumvent the "missing hydrogen" problem are shown in Figure 3, although each faces its own challenges. For instance, polyethylene chains could potentially grow by repeated ring expansion of a chromacycle (designated **M**),[15] or by alternation of carbene and chromacyclobutane intermediates (**C**).[16] Neither mechanism requires an external source of hydrogen or alkyl groups; however, results from isotopic labeling experiments[11,14] are not consistent with these mechanisms. Large propagation barriers for these mechanisms have also been computed using first-principles calculations.[13,17,18]

This study investigates yet three more polymerization mechanisms, none of which requires an external source of hydrogen or alkyl groups. First, the oxachromacycle mechanism (**O**) resembles the chromacycle mechanism, except that the ring includes a Cr–O bond. Second, we consider initiation by proton transfer from ethylene, followed by Cossee–Arlman polymerization at a ≡Si(OH)Cr(II)-vinyl site (**H2**).[19] For

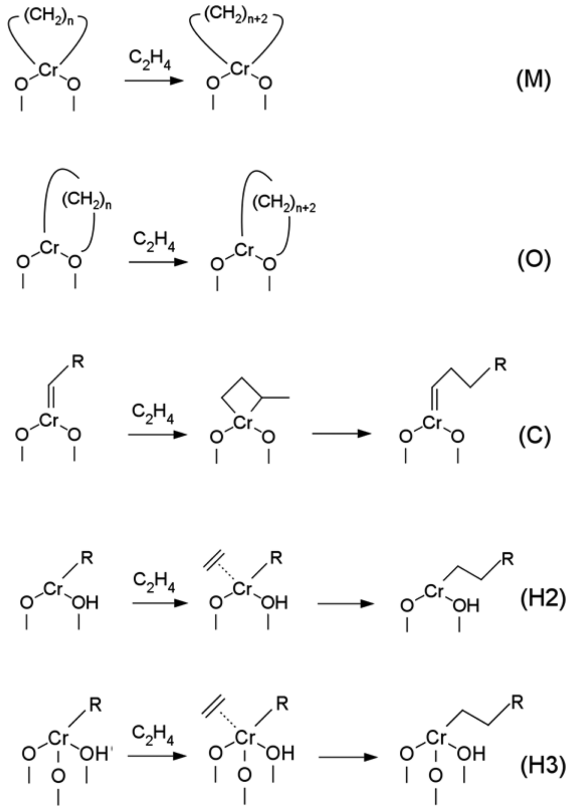

Figure 3. Five alternative propagation mechanisms proposed for ethylene polymerization by the Phillips catalyst. Chromacycle (M): ethylene inserts into either of two equivalent Cr–C bonds in a ring that includes a Cr(IV) ion. Oxachromacycle (O): polymer grows by insertion into the Cr–C bond of a ring that includes a support O and a Cr(II) ion. The ring is initially formed by addition of ethylene across a Cr–O bond. Carbene (C): an alkylidenechromium(IV) site undergoes ethylene cycloaddition to give a substituted chromacyclobutane, which then reverts to an alkylidene via a 1,3-H shift. Cossee–Arlman with Cr(II) (H2): ethylene inserts into the Cr–C bond of an alkylchromium(II) site with bridging OH. Cossee–Arlman with Cr(III) (H3): ethylene inserts into the Cr–C bond of an alkylchromium(III) site with bridging OH.

both of these mechanisms, the Cr oxidation state is 2+, consistent with the prereduced Phillips catalyst that initiates polymerization spontaneously without an induction period.[20,21] Finally, we also consider polymerization at an analogous Cr(III) site (**H3**). Delley et al. proposed initiation by proton transfer from ethylene, such as that shown for the Cr(II) (**H2** mechanism), to create a ≡Si(OH)Cr(III)-vinyl site,[22,23] at which a polymer chain grows by a Cossee–Arlman mechanism. Termination was suggested to occur via proton transfer back to the alkyl chain.

In this work, we also examine the five hypothetical mechanisms with a view to their kinetic competence. Specifically, we investigate the barriers to initiation, the kinetics of polymerization, the polymer molecular weight, and termination pathways that do and do not create a new site ready for polymerization. All mechanisms are examined with a single range-separated DFT model chemistry to enable direct comparisons. Although DFT does not provide chemical accuracy, we invoke typical errors from benchmark calculations (~20 kJ/mol)[24,25] to assess the plausibility or implausibility of proposed mechanisms.

DOI: 10.1021/acscatal.5b00016
ACS Catal. 2015, 5, 3360–3374

2. METHODS AND MODELS

All calculations were performed with Gaussian09.[26] Except where noted, energies, gradients, and Hessian matrices for all structures were calculated with the range-separated density functional, ωB97X-D,[27] which has been recommended on the basis of benchmarking studies for barrier heights[28−31] and geometries of transition metal catalysts.[32] The basis set used for Cr is def2-TZVP,[33,34] and the basis set used for C, H, O, and Si is TZVP.[35] Most of the analysis requires only approximate results to assess plausibility of different mechanisms. Section 3.8 includes a comparison to CCSD(T) results because there we estimate the polymerization rate. For all calculations, the highest spin contaminant was annihilated, as summarized in Table S1 of the Supporting Information. The geometries of all minimum-energy structures were optimized with the Berny algorithm[36] in Gaussian09. For convergence, the maximum and RMS forces were set to 4.50×10^{-4} and 3.00×10^{-4} Hartrees/Bohr, respectively, and the maximum and RMS displacements were set to 1.80×10^{-3} and 1.20×10^{-3} Bohr, respectively. Transition state structures were calculated using a memory-enhanced eigenvector-following algorithm.[37] The norm of the mass-weighted gradient was limited to 3.00×10^{-4} Hartrees/(Bohr·amu$^{1/2}$), and the tolerance for energy was 1.00×10^{-5} Hartrees. Finally, every converged transition state was required to have only one imaginary frequency. Thermal corrections were computed for the Gibbs' free energies of reaction and activation for all elementary steps. Gibbs' free energies include rotation, vibration, and translation[38] at the experimentally relevant operating temperature of 373.15 K (Table S2).[1,2,39] Free energies for gaseous species were calculated at the standard state pressure of 1 atm.

The Cr(II) active site precursor was modeled as the energy-minimized bis(silanolato)chromium(II) cluster shown in Figure 4 and Table 1. This structure represents the product of

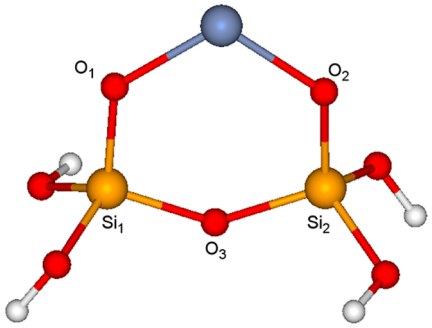

Figure 4. Structure of the optimized Cr(II) cluster **^{5}I**. Color scheme: Cr (blue), O (red), Si (orange), H (white).

chromate ester reduction by either CO or ethylene.[18,20,40,41] In the optimized, quintuplet-spin ground state of the cluster model, Cr(II) is bonded to two silanolate oxygens at a distance of 1.82 Å. A third bridging oxygen is located between the two silicon atoms to complete a six-membered chromasiloxane ring. Finally, the silicon atoms are capped with hydroxyl groups, whose positions were optimized in the original cluster then fixed in all subsequent calculations. This anchoring of the terminal hydroxyl groups approximates the rigidity of the solid catalyst support. The structure of the final cluster is similar to one used in a previous computational study by Espelid and Børve;[13] however, our O−Cr−O and Si−O−Si angles (109.8 and 139.3°) are considerably smaller than those chosen

Table 1. Key Interatomic Distances (Å) and Bond Angles (deg) for the Cr(II) Cluster ^{5}I and Cr(III) Cluster ^{4}H3.I

		^{4}H3.I	
parameter	^{5}I[a]	ωB97X-D	B3LYP-D3[b]
*r*Cr−O1	1.82 (1.82)	1.791	1.805 (1.805)
*r*Cr−O4		1.781	1.798 (1.798)
∠O1−Cr−O2	110 (116)	104	103
∠O1−Cr−O4		114	113
∠Cr−O1−Si1	127	125	126
∠Cr−O4−Si3		130	132
∠Si1−O3−Si2	139	132	132
∠Si1−O6−Si5		137	139

[a]Values in parentheses computed by Espelid and Børve.[13] [b]Values in parentheses computed by Delley et al.[23]

previously (116 and 141−147°). Although average Si−O−Si angles in amorphous silicas are typically 148−152°,[42,43] Demmelmaier et al. found that Phillips active sites are associated with strained chromasiloxane rings, such as the 6-membered ring used here.[44]

To evaluate the mechanism recently proposed by Delley et al.[22,23,45] and to facilitate direct comparison with the published results, we also used the tris(silanolato)chromium(III) cluster model **^{4}H3.1** (Figure 5 and Table 1). The cluster consists of a

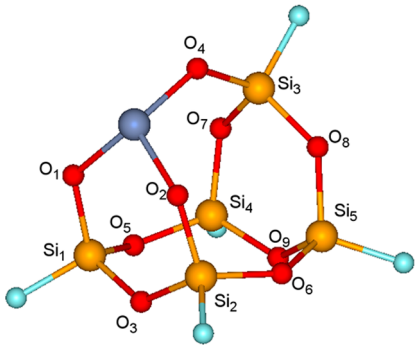

Figure 5. Structure of the optimized Cr(III) cluster **^{4}H3.I**. Color scheme: Cr (dark blue), O (red), Si (orange), F (light blue).

six-membered chromasiloxane ring connected through three oxygen bridges to a second six-membered siloxane ring. The results were computed with the same ωB97X-D functional used for **^{5}I**, with the def2-TZVP basis set for Cr and TZVP basis set for C, H, O, Si, and F. To reproduce the published B3LYP calculations[46,47] and to investigate additional termination pathways, structures were optimized with the LANL2DZ[48−50] basis set for Cr and 6-311G(d,p)[51,52] basis set for C, H, O, Si, and F with energy refinement using the LANL2TZ(f)[48,53,54] basis set for Cr and 6-311++G(d,p)[51,52,55] basis set for C, H, O, Si, and F. Dispersion correction was also included, using Grimme's DFT-D3 with Becke−Johnson damping.[56,57] Finally, all free energies were calculated at 373.15 K and 1 atm, although results at 298.15 K are also provided in Table S3 for comparison with the previous DFT study.[23]

An obvious difference between the two cluster models, **^{5}I** and **^{4}H3.I**, is their treatment of capping groups. Following Delley et al.,[23] we report results for an F-terminated cluster model with no constraints on the F atoms. We adopted their cluster modeling procedures to ensure that differences in our results emerge from the pathways included and the analyses of the

DOI: 10.1021/acscatal.5b00016
ACS Catal. 2015, 5, 3360−3374

DFT results, not from differences in the cluster model. However, we also note that the choice of capping groups and constraints should have small effects. Constraint effects are expected to be minor because the cluster geometry is already rigid owing to its five edge-sharing rings. Moreover, −OSi− bridges should largely shield the Cr center from electronic differences between F and OH capping atoms. We checked these assumptions with additional calculations using two alternative versions of the ^{4}**H3.I** cluster. Both of the alternative cluster models used hydroxyl capping groups in place of the fluorine atoms. Key energy differences and activation energies for F-terminated and OH-terminated clusters, with and without capping atom constraints, are compared in the Supporting Information (Table S4).

All calculated minimum-energy species are named using the notation $^{\#}$X.Y, where # is the spin multiplicity, X denotes the mechanism, and Y is a Roman numeral. For instance, ^{5}**M.IV** refers to the fourth quintuplet-spin species in the metallacycle mechanism. ^{3}**M.IV** refers to the same structure reoptimized with a triplet spin multiplicity. Some species appear in multiple mechanisms, such as ^{5}**I** (Figure 4), which refers to the initial Cr(II) species in a quintuplet spin state. Thus, the name for this bare site does not include an X designation. Transition states are described using a similar notation, $^{\#}$TS[X.Y_1-X.Y_2], where TS denotes a transition state structure and Y_1 and Y_2 refer to reactant and product, respectively.

Some results in this present paper pertain to mechanisms studied computationally by others.[13,17,18,58] The ωB97X-D functional we used here is more accurate relative to what was available and feasible at the time of their studies.[28−31] Furthermore, we analyzed alternate spin states and computed free energy barriers, which allows us to estimate rates of reactions. Nevertheless, the general agreement between their findings and ours, where overlap exists, adds confidence both to the previous conclusions and to our results for the new mechanisms.

3. RESULTS AND DISCUSSION

3.1. Ethylene Binding to the Bare Cr(II) Site. Prior to polymerization, ethylene can form several different coordination complexes with the bare Cr(II) site ^{5}**I** (Figure 6). The quintuplet-spin complex ^{5}**II** is formed when ethylene binds trans to one of the silanolate ligands. The C−C bond is elongated by only 0.02 Å, at a Cr−C distance of 2.40 Å. The structural parameters, summarized in Table S5, compare well with previous computational results reported by Espelid and Børve;[13] however, the binding energy of −84 kJ/mol calculated here differs from their −68 kJ/mol. Our calculations use different functionals (ω-B97X-D vs BVP86),[59,60] different terminal capping groups (OH vs H), and a different ring geometry. The O−Cr−O angle, which appears to be crucial in Phillips site activation,[44] is slightly smaller (104 vs 107°). We compute a smaller energy change of only −65 kJ/mol for ethylene binding to an eight-membered chromasiloxane ring with a much larger O−Cr−O angle (135°) (Figure S1 and Table S6).

The free energy change for binding the first ethylene to ^{5}**I** is −24 kJ/mol at 373 K; coordination of a second ethylene occurs with a free energy change of only −9 kJ/mol (^{5}**III**). This weaker interaction is reflected in an increase in the average Cr−C distance, from 2.40 Å in ^{5}**II** to 2.48 Å in ^{5}**III** (Table S5). Steric crowding around the metal appears to hinder further ethylene binding; a stationary point for a third coordinated

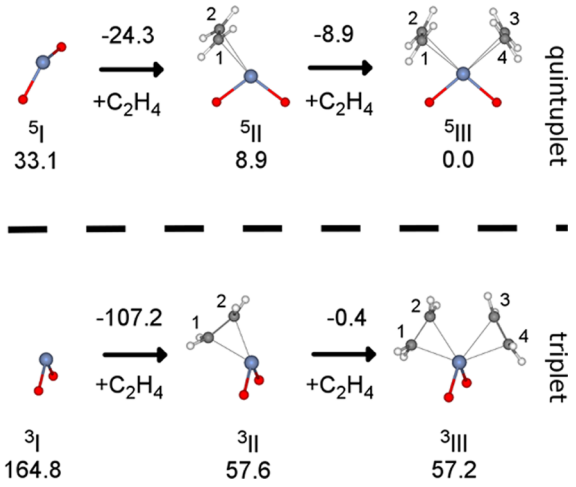

Figure 6. Structures for ethylene complexes of the Cr(II) cluster, as well as their free energies (kJ/mol) relative to the most stable bis(ethylene) complex, ^{5}**III**, at 373 K. Numbers above arrows correspond to reaction free energies. Si atoms and the rest of the siloxane cluster are omitted for clarity. ^{5}**I**, bare Cr(II) site; ^{5}**II**, mono(ethylene) complex; ^{5}**III**, bis(ethylene) complex; as well as corresponding triplet structures and energies. Color scheme: Cr (blue), O (red), H (white), C (gray).

ethylene was not found, although weakly bound tris- and tetrakis(ethylene) complexes have been reported with Cr-(OH)$^{+}$ and other models with considerably smaller ligand sets.[58,61] Therefore, the bis(ethylene) complex ^{5}**III** is the most likely stable intermediate present prior to initiation of polymerization for this model. It also represents the reference point of free energy, unless otherwise noted.

For both mono and bis(ethylene) complexes ^{5}**II** and ^{5}**III**, higher energy analogs with triplet spins (^{3}**II** and ^{3}**III**) also exist (Figure 6). For instance, ^{3}**III** is 57 kJ/mol higher in free energy than ^{5}**III**. They also differ in the orientation of the ethylenes relative to the OCrO plane. These species are not considered further, except where noted.

3.2. Chromacycle Expansion Mechanism (M). Homogeneous organochromium catalysts have been reported to oligomerize ethylene via a metallacycle mechanism[62,63] in which ethylene inserts repeatedly into an expanding ring system that includes the Cr ion.[64] Because the ring always contains an even number of H atoms, no external source of H is required. In the absence of discernible vibrations attributable to terminal $-CH_3$ groups, Groppo et al. assigned the observed IR bands to $-CH_2-$ groups of an expanding chromacycle;[65] however, $-CH_3$ bands can be difficult to detect for long chain lengths. McGuinness et al. examined isotopomers obtained from copolymerizing ethylene with isotopically labeled decenes and concluded that a chromacycle mechanism is unlikely.[11]

Chromacycle ring expansion was modeled starting with a chromacyclopentane ring, formed by cycloaddition of the two coordinated ethylenes in ^{5}**III**.[13,18] The most stable form of this ring has a triplet spin configuration (^{3}**M.IV** in Figure 7), with a free energy of +9 kJ/mol relative to ^{5}**III**. Free energies for the quintuplet and singlet spin forms are significantly higher, at 101 and 156 kJ/mol, respectively. This preference for the triplet spin state in the metallacycle raises the issue of spin conservation because the initial state is the quintuplet-spin bis(ethylene) complex ^{5}**III**. The question was addressed in previous computational work on the model ethylene dimeriza-

DOI: 10.1021/acscatal.5b00016
ACS Catal. 2015, 5, 3360−3374

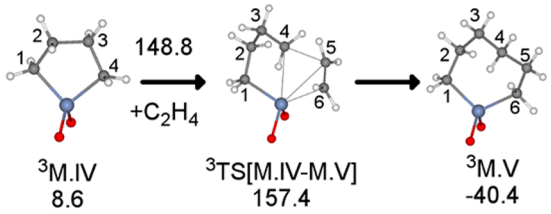

Figure 7. Structures of stationary points in the chromacycle mechanism and free energies (kJ/mol) relative to the bis(ethylene) complex, ^{5}**III**, at 373 K. ^{3}**M.IV**, chromacyclopentane; ^{3}**TS**[**M.IV-M.V**], transition state for insertion of ethylene into the Cr−C4 bond; ^{3}**M.V**, chromacycloheptane.

tion catalyst ($Cr(OH)^+$), which also prefers different spins in the corresponding chromacycle and bis(ethylene) complexes.[58] In that case, spin crossover to the triplet state was assumed to precede metallacycle formation. However, because subsequent propagation via chromacycle expansion is extremely slow (vide infra), effectively ruling out this mechanism, we did not attempt to optimize the minimum on the seam of crossing, an essential part of the required initiation step.

In the late transition state ^{3}**TS**[**M.IV-M.V**], the Cr−C4 distance increases dramatically, from 1.99 to 2.99 Å, to accommodate the incoming monomer (Table S7). This elongated distance compares well with the 3.02 Å reported by Zhong et al.[18] but contrasts with the much smaller value of 2.21 Å reported by Espelid and Børve.[13] Nevertheless, all calculated activation energies are large: 112,[18] 119,[13] and 89 kJ/mol (this work). Upon including the loss of entropy of the free ethylene molecule, we obtain a prohibitively large total free energy barrier of 149 kJ/mol, resulting in a rate constant of only 1×10^{-8} s^{-1} $site^{-1}$ atm^{-1} at T = 373 K. Although the chromacycloheptane product ^{3}**M.V** is 49 kJ/mol lower in free energy relative to ^{3}**M.IV**, the high insertion barrier shows that the chromacycle mechanism (**M**) is not a viable route for polymer chain growth.

Despite the impracticality of ring expansion as a polymerization mechanism, Espelid and Børve postulated a chromacycle as a relevant intermediate in side-reactions.[13] They suggested that any chromacycloheptane that does form may undergo intramolecular β-H transfer to give 1-hexene, since this would be faster than subsequent ethylene insertion (activation energies of 98 vs 122 kJ/mol, respectively). The fast termination might explain reports of 1-hexene formed in polymerization experiments with the Phillips catalyst.[66,67] Such reactions have been widely observed with homogeneous chromium catalysts that trimerize ethylene selectively.[62,68,69] We find similar trends in the activation energies for termination versus a second ethylene insertion (114 and 129 kJ/mol, respectively). The difference is even larger in the free energy barriers for β-H transfer and insertion: 114 and 189 kJ/mol, respectively (Figure 8, with geometries in Table S8).

Nevertheless, the very slow rate we calculate for ring expansion of the chromacyclopentane suggests that even chromacycloheptane is unlikely to form on this type of site. Espelid and Børve noted that the activation energy for ethylene insertion on a model chromacyclopentane decreases by 46 kJ/mol, to 73 kJ/mol, when Cr is part of a four-membered chromasiloxane ring with a very small, strained O−Cr−O angle.[13] At the same time, the termination barrier also decreases, but only by 13 kJ/mol, to 85 kJ/mol. However, including the entropy of immobilizing the free monomer prior

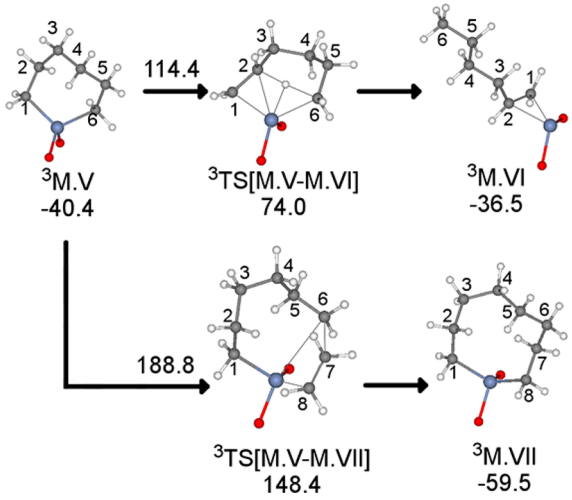

Figure 8. Structures of stationary points in chromacycle propagation and termination by β-H transfer, and free energies (kJ/mol) relative to the bis(ethylene) complex, ^{5}**III**, at 373 K. ^{3}**M.V**, chromacycloheptane; ^{3}**TS**[**M.V-M.VI**], transition state for intramolecular β-H transfer; ^{3}**M.VI**, coordinated 1-hexene; ^{3}**TS**[**M.V-M.VII**], transition state for ethylene insertion into the Cr−C6 bond; ^{3}**M.VII**, chromacyclononane.

to the insertion step leads to a free energy of activation for ring expansion that is still larger than that of termination. Nevertheless, rare sites similar to the four-membered ring studied by Espelid and Børve may be responsible for the coproduction of α-olefins, suggesting that a future analysis of structure sensitivity in the active sites may be fruitful.

3.3. Oxachromacycle Expansion Mechanism (O). This mechanism is adapted from one originally suggested by Baker and Carrick for a homogeneous polymerization catalyst, bis(triphenylsilyl)chromate.[70] In that system, the first ethylene insertion was suggested to occur at one of the two Cr−O bonds (eq 1), followed by ethylene insertion into the resulting Cr−C bond. To the best of our knowledge, the viability of such a mechanism has not been evaluated computationally for the heterogeneous Phillips catalyst.

$$(Ph_3SiO)_2Cr + nC_2H_4 \rightarrow Ph_3SiOCr(CH_2CH_2)_nOSiPh_3 \quad (1)$$

The reaction is initiated from the bis(ethylene) complex ^{5}**III** when a coordinated ethylene adds to the Cr−O1 bond (Figure 9). In contrast to Baker and Carrick's proposal, we find that the Cr−O1 bond does not break, although the distance lengthens from 1.88 to 1.96 Å (Table S9). Instead, O1 becomes tricoordinate (Cr, C, Si), forming the oxachromacyclobutane intermediate ^{5}**O.IV**. Upon addition, the ethylene becomes distorted toward a nonplanar geometry, indicating increased sp^3 character at its carbon atoms. Furthermore, the Cr−C2 and O1−C1 frequencies in structure ^{5}**O.IV** are 467 and 809 cm^{-1}, respectively, suggesting the formation of strong bonds. However, the Cr−O1 bond in ^{5}**O.IV** also has a vibrational frequency 467 cm^{-1}, indicating that a relatively strong Cr−O1 bond remains. Overall, the initiation step associated with the late transition state ^{5}**TS**[**III**−**O.IV**] occurs with an activation free energy of 81 kJ/mol and a reaction free energy of 68 kJ/mol. In the oxachromacycle, the Cr(II) site remains a quintuplet, so no change in spin state is required. Because the triplet and singlet configurations for the ethylene−oxachromacyclobutane complex **O.IV** are 144 and 320 kJ/

DOI: 10.1021/acscatal.5b00016
ACS Catal. 2015, 5, 3360−3374

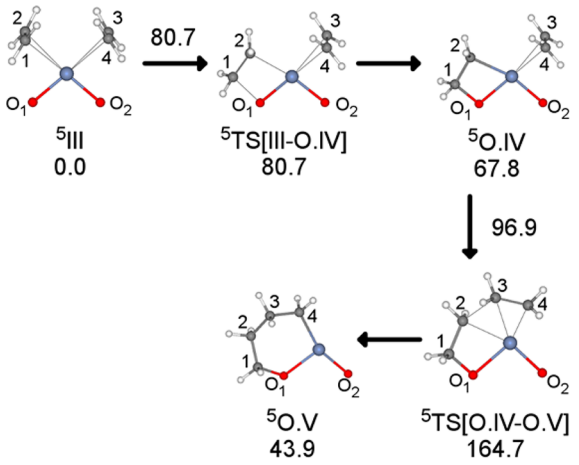

Figure 9. Stationary points for the oxachromacycle mechanism and free energies (kJ/mol) relative to that of the bis(ethylene) complex ^{5}**III**, at 373 K. ^{5}**TS**[**III**−**O.IV**], transition state for ethylene insertion into the Cr−O bond; ^{5}**O.IV**, ethylene−oxachromacyclobutane complex; ^{5}**TS**[**O.IV-O.V**], transition state for ethylene insertion into the Cr−C2 bond; ^{5}**O.V**, oxachromacyclohexane.

mol higher in energy relative to ^{5}**III**, reaction paths relevant to their corresponding spins were not considered further.

For quintuplet ^{5}**O.IV**, the remaining bound ethylene ligand inserts into the newly formed Cr−C2 bond to form the oxachromacyclohexane ^{5}**O.V** (Table S10). The barrier is 97 kJ/mol (corresponding to k = 0.2 s^{-1} atm^{-1} $site^{-1}$ at 373 K), which is significantly lower than the insertion barrier for the chromacyclopentane ^{3}**M.IV** (149 kJ/mol, see Figure 7). This may be a consequence of lower steric hindrance in ^{5}**O.IV** due to the smaller Cr coordination number. However, because the preceding step (^{5}**III** → ^{5}**O.IV**) is endothermic, the effective barrier to transform ^{5}**III** into ^{5}**O.V** is 165 kJ/mol, corresponding to a very low effective rate constant of 7 × 10^{-11} s^{-1} atm^{-1} $site^{-1}$ at 373 K. Thus, our calculations suggest that the oxachromacycle is not a viable intermediate for polymerization. However, the free energy to create the oxachromacycle as well as later polymerization steps may be quite sensitive to the local support geometry. Further analyses of this mechanism for cluster models of varying geometry are needed for a more definitive conclusion.

3.4. Green−Rooney (Carbene) Mechanism (C). In principle, polymer chain growth can be accomplished by an olefin metathesis-type mechanism involving alternating carbene and substituted chromacyclobutane intermediates, also known as the Green−Rooney mechanism.[71] A version adapted for the Phillips catalyst is depicted in Figure 10. Because all of the intermediates have an even number of hydrogen atoms, this mechanism also avoids the missing hydrogen problem. Although exceedingly rare in molecular catalysis,[72,73] the Green−Rooney mechanism was proposed for the Phillips catalyst by Kantcheva et al.[16] on the basis of IR signals assigned to the Cr=C and C−H methyl stretches of an ethylidene intermediate, such as ^{3}**C.IV**. Nait Ajjou and Scott prepared a silica-supported bis(neopentyl)chromium(IV) catalyst that undergoes α-H elimination to give a neopentylidene complex capable of initiating ethylene polymerization.[66] Furthermore, olefins with an odd number of carbons, which may arise from olefin metathesis over a carbene intermediate, were detected during the early stages of reaction over a Phillips catalyst.[74,75]

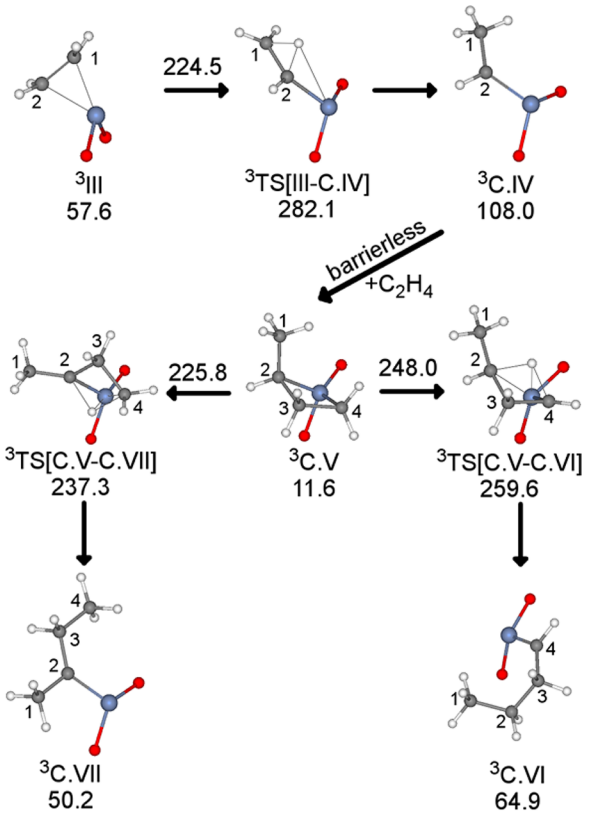

Figure 10. Structures of stationary points in the Green−Rooney (carbene) mechanism and free energies (kJ/mol) relative to that of the bis(ethylene) complex ^{5}**III** at 373 K. ^{3}**TS**[**C.III-C.IV**], transition state for 1,2-H transfer from C2 to C1; ^{3}**C.IV**, ethylidenechromium; ^{3}**C.V**, (2-methyl)chromacyclobutane; ^{3}**TS**[**C.V**−**C.VI**], transition state for 1,3-H transfer from C4 to C2; ^{3}**C.VI**, butylidenechromium; ^{3}**TS**[**C.V-C.VII**], transition state for 1,3-H transfer from C2 to C4; ^{3}**C.VII**, (1-methyl)propylidenechromium.

The initiating ethylidenechromium(IV) site ^{3}**C.IV** could form by rearrangement of the bound ethylene ligand in ^{3}**III**, resulting in a change in formal oxidation state from Cr(II) to Cr(IV). We calculate a barrier for this step of 225 kJ/mol, similar to the 214 kJ/mol reported by Zhong et al.[18] Like the chromacycle ^{3}**M.IV**, a triplet spin state is preferred for ^{3}**C.IV**. Relative to ^{5}**III**, the free energy of ^{3}**C.IV** and free monomer (included for stoichiometry) is a high 108 kJ/mol (geometries in Table S11). Quintuplet and singlet spin configurations are 151 and 234 kJ/mol higher in free energy relative to ^{5}**III**, respectively.

Chain propagation, which involves [2 + 2] cycloaddition of ethylene followed by intramolecular 1,3-H-transfer within the chromacyclobutane intermediate, is slow overall. The first step, which generates the substituted metallacycle ^{3}**C.V**, is barrierless and has a favorable free energy change of −96 kJ/mol, but subsequent H-transfer to generate one of two possible carbenes, ^{3}**C.VI** or ^{3}**C.VII**, is predicted to be extremely sluggish. For instance, when H is transferred from the unsubstituted α-carbon (C4) of ^{3}**C.V** to the methyl-substituted α-carbon (C2), the barrier is an enormous 248 kJ/mol (^{3}**TS**[**C.V-C.VI**] in Figure 10). Several previous computational studies reported similarly high barriers, in the range 231−241 kJ/mol.[13,17] The alternative, H transfer from C2 to C4 to give (1-methyl)propylidene ^{3}**C.VII**, is slow, as well. The free energy change for the reaction is 39 kJ/mol, with a barrier of 226 kJ/

DOI: 10.1021/acscatal.5b00016
ACS Catal. 2015, 5, 3360−3374

mol. The slightly lower values, relative to those for the path to generate the butylidenechromium ^{3}**C.VI**, are due to the increased stability of the more substituted carbene ^{3}**C.VII**. Nevertheless, the high barriers for both H-transfer reactions show that propagation of polymerization by the Phillips catalyst is unlikely to involve a carbene intermediate. Geometries for intermediates in both pathways are compiled in Tables S12, S13.

These findings are consistent with a previous experimental study in which the expected H/D scrambling for polymerization of CHD═CHD by a Green−Rooney mechanism was not observed.[14] The resulting polymer contained only [CHD] units, although the Green−Rooney mechanism should cause scrambling of the isotopic label (producing CH_2 or CD_2 units) via H/D transfer in the transition state (Figure 11).

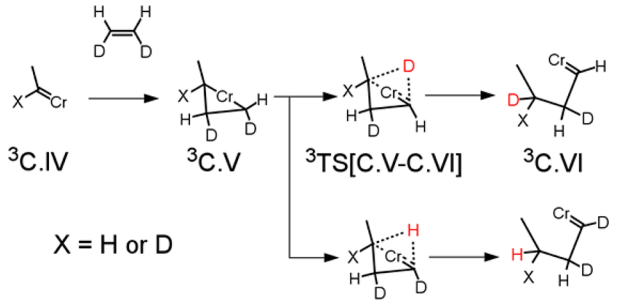

Figure 11. Green−Rooney mechanism for polymerization of *cis*-ethylene-l,2-d_2, showing the expected scrambling of the isotope label. This scrambling is not observed for the Phillips catalyst.

Furthermore, only small kinetic isotope effects have been reported for C_2D_4 polymerization.[11,76] A sizable primary effect is expected for the Green−Rooney mechanism because the rate-determining step involves H/D transfer in the transition states ^{3}**TS**[**C.V-C.VI**] and ^{3}**TS**[**C.V-C.VII**].

3.5. Cossee−Arlman Chain Growth at a Monoalkylchromium(II) Site Initiated by Proton Transfer from Ethylene (H2).

In contrast to the metallacycle and oxametallacycle mechanisms described above, the growing polymer chain in a Cossee−Arlman mechanism[8] is covalently bonded to the active site at only one end. A coordinated monomer inserts into this Cr−C σ-bond to extend the length of the polymer chain. To maintain an even number of H atoms in the active site and thereby avoid the missing hydrogen problem, Delley et al. suggested initiation by proton transfer from one of the ethylene ligands in ^{5}**III** to a silanolate oxygen.[19] A mechanism involving this type of proton transfer on the Cr(II) precatalyst is shown in Figure 12, creating the vinyl ligand in ^{5}**H2.V**. The growing alkyl ligand attached to Cr(II) is terminated by a vinyl end group, $-(CH_2CH_2)_nCH{=}CH_2$. A similar proton transfer initiation pathway involving Cr(III)/SiO_2 was investigated by Delley et al.;[23] the Cr(III) case will be analyzed in section 3.6 below.

The free energy barrier for proton transfer to create the ≡Si(OH)Cr^{II}-vinyl site is 126 kJ/mol, and the free energy of the site ^{5}**H2.V** is +85 kJ/mol relative to ^{5}**III** (geometries in Table S14). Like the other Cr(II) species considered in this study, its preferred spin multiplicity is quintuplet. Triplet and singlet forms have much higher energies (176 and 246 kJ/mol, respectively).

Propagation proceeds by monomer insertion into the Cr−C σ-bond. At the transition state ^{5}**TS**[**H2.V-H2.VIa**], the Cr−C2

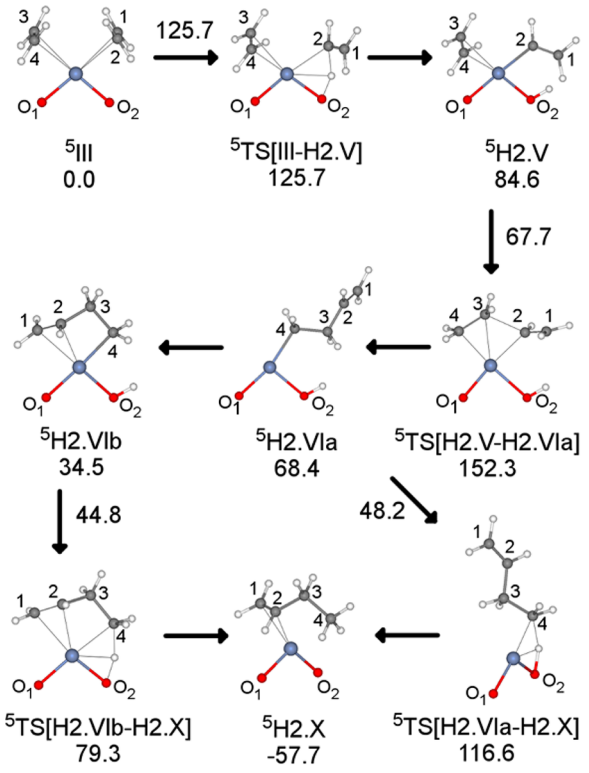

Figure 12. Stationary points for the Cossee−Arlman mechanism on a Cr(II) site, and free energies (kJ/mol) relative to that of the bis(ethylene) complex ^{5}**III**, at 373 K. ^{5}**TS**[**III-H2.V**], transition state to transfer H to O2; ^{5}**H2.V**, (ethylene)(vinyl)chromium(II); ^{5}**TS**-[**H2.V-H2.VIa**], transition state for ethylene insertion into the Cr−C2 bond; ^{5}**H.VIa**, butenylchromium(II) with uncoordinated vinyl chain end; ^{5}**H2.VIb**, butenylchromium(II) with coordinated vinyl chain-end; ^{5}**TS**[**H2.VIb-H2.X**], transition state for H transfer from O2 to C4, with coordinated vinyl end group; ^{5}**H2.X**, 1-butene complex; ^{5}**TS**-[**H2.VIa-H2.X**], transition state for H transfer from O2 to C4 without vinyl end group coordination.

bond of ^{5}**H2.V** stretches slightly, from 2.09 to 2.13 Å (Table S15), while incipient Cr−C4 and C2−C3 bonds appear at 2.12 and 2.02 Å, respectively. The reaction and activation free energies for formation of the butenylchromium(II) intermediate ^{5}**H2.VIa** are −16 and +68 kJ/mol, respectively, relative to ^{5}**H2.V**; however, the transition state ^{5}**TS**[**H2.V-H2.VIa**] is a high 152 kJ/mol relative to the stable starting point ^{5}**III**, suggesting that overall formation of ^{5}**H.VIa** from ^{5}**III** would be extremely slow ($k = 4 \times 10^{-9}$ s^{-1} $site^{-1}$) at 373 K.

If a faster initiation path to ^{5}**H.VIa** were accessible, the low ethylene insertion barrier of 68 kJ/mol might suggests that polymer chains could be formed via a Cossee−Arlman mechanism at these sites. The next ethylene insertion also has a low free energy barrier of 86 kJ/mol (Figure S2 and Table S16). However, growth at this Cr^{II}-alkenyl site is not viable, because ^{5}**H2.VIa** favors chain termination prior to additional monomer insertion. The butenyl ligand can coordinate to Cr(II) via its vinyl end-group (^{5}**H2.VIb**), while the bridging silanol prepares to transfer H back to C4, causing the Cr−C σ-bond to break in ^{5}**TS**[**H2.VIb-H2.X**] (Table S17). The resulting coordinated 1-butene complex ^{5}**H2.X** is formed with reaction and activation free energies of −92 and 45 kJ/mol, respectively. When the vinyl end is not coordinated to Cr(II), it models the behavior of a much longer polymer chain whose bending and attachment to Cr comes at the expense of

DOI: 10.1021/acscatal.5b00016
ACS Catal. 2015, 5, 3360−3374

configurational entropy. In this case, H transfer to C4 (^{5}**TS**[**H2.VIa-H2.X**]) occurs with a slightly higher barrier of 48 kJ/mol. Since the propagation barrier (~80 kJ/mol) is much higher than either termination barrier, this active site cannot account for the formation of long polymer chains by the Phillips catalyst.

Formation of an ethoxy complex such as ^{5}**H2.IX** by ethylene insertion into the O−H bond of the coordinated silanol of ^{5}**H2.V** (Figure 13) would effectively prevent silanol proton

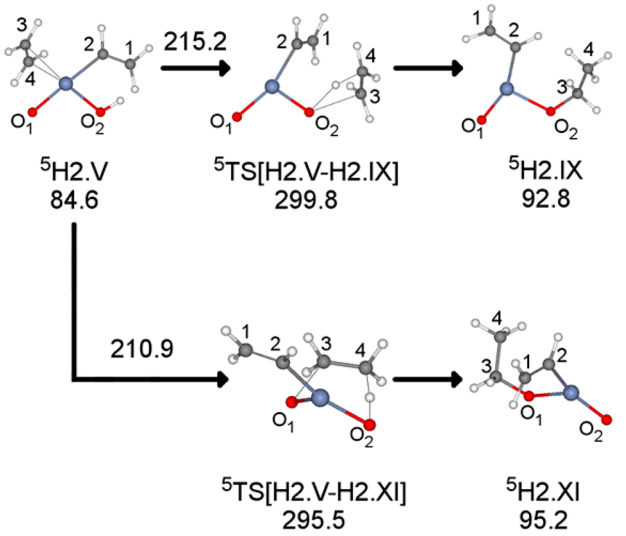

Figure 13. Stationary points for formation of a bridging ethoxy ligand adjacent to a vinylchromium(II) site, and free energies (kJ/mol) relative to that of the bis(ethylene) complex ^{5}**III**, at 373 K. ^{5}**H2.V**, (ethylene)(vinyl)chromium; ^{5}**TS**[**H2.V-H2.IX**], transition state to form ethoxy at O2; ^{5}**H2.IX**, (ethoxy)(vinyl)chromium with ethoxy at O2; ^{5}**TS**[**H2.V-H2.XI**], transition state to form ethoxy at O1; ^{5}**H2.XI** (ethoxy)(vinyl)chromium with ethoxy at O1.

migration and the ensuing termination of the growing polymer chain. Olefin insertion into the O−H bonds of bridging hydroxyls is well-known in zeolites.[77] Unfortunately, although the ethoxy complex is only 8 kJ/mol higher in energy relative to ^{5}**H2.V**, the barrier to its formation is a prohibitive 215 kJ/mol in ^{5}**TS**[**H2.V-H2.IX**] (Table S18). To explore the effect of ring strain, the energy of a transition state with a larger ring, ^{5}**TS**[**H2.V-H2.XI**], was also calculated. Unfortunately, it is similarly very high in free energy (Figure 13).

3.6. Cossee−Arlman Chain Growth at a Monoalkylchromium(III) Site Initiated by Proton Transfer from Ethylene (H3). The tendency of Cr(II) sites in the Phillips catalyst to catalyze ethylene oligomerization rather than polymerization was reported by Theopold,[78] who found only propylene and other short-chain α-olefins in the solution-phase reaction of Cp*Cr^{II}(dmpe)Me [dmpe = bis(dimethylphosphino)ethane] with ethylene. On the other hand, a cationic Cr(III) analog, [Cp*Cr^{III}(dmpe)Me]PF$_6$, was shown to be capable of ethylene polymerization. These results suggest that the Phillips active site has an oxidation state higher than II, even though Cr(II) sites may be the immediate precursors of these sites. Merryfield et al. observed oxidation of Cr(II) upon exposure of a Phillips catalyst to ethylene.[20]

Recently, Delley et al. prepared a Cr(III)/SiO$_2$ catalyst for which they proposed initiation by ethylene deprotonation,[23] similar to that described for the Cr(II) site in the previous section. In support of this hypothesis, they assigned new IR peaks at 3605 and 3640 cm^{-1} to the O−H stretching of the proposed (≡SiO)$_2$(OH)Cr^{III}-alkyl active sites. Although they performed DFT calculations for the initiation, propagation, and termination steps (using the B3LYP-D3 functional with a triple-ζ basis and pseudopotentials), they did not use their results to predict the overall rate, polymer molecular weight, or abundance of propagating sites. The abundance is particularly important because it bears on whether their spectroscopic assignments are plausible; only sites with non-negligible abundances are observable. In this section, we present these informative kinetic analyses, in addition to our own, independent DFT results. Our calculations using the ωB97X-D functional are very similar to the reported[23] results obtained using B3LYP-D3 (Table S3). Although the earlier study reported Gibbs free energies at 298 K, we present results at a typical catalyst operation temperature, 373 K, except where needed for comparison to the previous work.

Compared with the Cr(II) model ^{5}**II**, the Cr(III) model ^{4}**H3.I** binds ethylene less strongly. With ωB97X-D, the bis(ethylene) complex ^{4} **H3.III** is 11 kJ/mol less stable than the mono(ethylene) complex ^{4} **H3.II** at 373 K (Figure 14). However, proton transfer in the mono(ethylene) complex ^{4}**TS**[**H3.II-H3.IV**] is prohibitively slow, with a barrier of 176 kJ/mol. Ethylene-assisted initiation is slightly more favorable, with a barrier of 151 kJ/mol from the bis(ethylene) complex (^{4}**H3.III** → ^{4}**TS**[**H3.III-H3.V**] → ^{4}**H3.V**). This corresponds to rate coefficients for proton transfer from ethylene, k_{init}, and its reverse, $k_{reverse}$, of 5×10^{-9} and 4×10^5 site^{-1} s^{-1}, respectively, at 373 K. Thus, like the Cr(II) case described in the previous section, the Cr(III) site initiates very slowly through proton transfer. The Cr−O1 bond stretches from 1.83 to 1.96 Å (Table S19). The remaining π-bound ethylene in ^{4}**H3.V** then inserts with a barrier of 37 kJ/mol (^{4}**TS**[**H3.V-H3.VIa**]). Geometries are summarized in Table S20.

Propagation for the Cr(III) site (Figure 15) is very similar to that for Cr(II). First, butenylchromium(III) ^{4}**H3.VIa** binds ethylene, forming the complex ^{4}**H3.VII**. Coordination is weak: the free energy change is +16 kJ/mol; $K_{bind} = 6 \times 10^{-3}$ atm^{-1} site^{-1}. Ethylene binding causes a distortion of the cluster model in ^{4}**H3.VII**, causing the nonbonded Cr−O8 distance (refer to Figure 5 and ^{4}**H3.I** in Figure 14) to shrink from 3.68 Å in ^{4}**H3.VIa** to 3.12 Å in ^{4}**H3.VII** (Table S21). The distance increases to 3.80 Å in ^{4}**TS**[**H3.VII-H3.VIII**] as ethylene inserts into the Cr−C4 bond, yielding hexenylchromium(III) ^{4}**H3.VIII**. The free energy barrier of 67 kJ/mol corresponds to a rate coefficient for ethylene insertion, k_{insert}, of 3×10^3 site^{-1} s^{-1}. The overall free energy difference between ^{4}**TS**[**H3.VII-H3.VIII**] and ^{4}**H3.VIa** is 83 kJ/mol.

Delley et al. considered several possible termination mechanisms from sites such as ^{4}**H3.VIa**, and concluded that the most favorable involves unassisted proton transfer from O1 to C4 of the growing chain (Figure 16, middle path, ^{4}**H3.VIa** → ^{4}**TS**[**H3.VIa-H3.Xa**] → ^{4}**H3.Xa**). This particular reaction mimics the reverse of initiation from a mono(ethylene) complex (Figure 14, ^{4}**H3.IV** → ^{4}**TS**[**H3.IV-H3.II**] → ^{4}**H3.II**), except that the product olefin in ^{4}**H3.Xa** interacts weakly with chromium through its methyl end rather than its vinyl end (geometries in Table S22). The free energy barrier from ^{4}**H3.VIa** is 99 kJ/mol ($k_{H\text{-}Xfer} = 9 \times 10^{-2}$ site^{-1} s^{-1}), which is slightly higher than the overall propagation barrier of 83 kJ/mol. The authors concluded that polymer chains could form by

DOI: 10.1021/acscatal.5b00016
ACS Catal. 2015, 5, 3360−3374

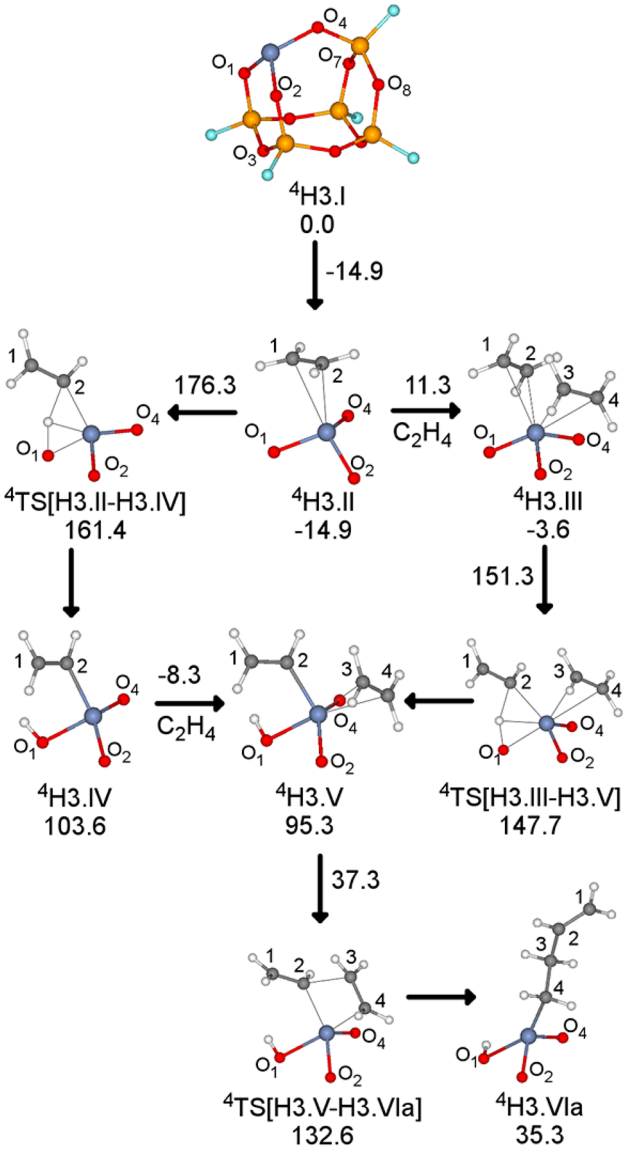

Figure 14. Stationary points for the Cossee–Arlman mechanism on a Cr(III) site and free energies (kJ/mol) relative to that of the bare site, ^{4} **H3.I**, at 373 K. ^{4} **H3.II**, mono(ethylene) complex; ^{4} **H3.III**, bis(ethylene) complex; ^{4}**TS**[**H3.II-H3.IV**], transition state to transfer H to O1 from mono(ethylene) complex; ^{4} **H3.IV**, vinylchromium-(III); ^{4}**TS**[**H3.III-H3.V**], transition state to transfer H to O1 from bis(ethylene) complex; ^{4} **H3.V**, (ethylene)(vinyl)chromium(III); ^{4}**TS**-[**H3.V-H3.VIa**], transition state for ethylene insertion into the Cr–C2 bond; ^{4} **H3.VIa**, butenylchromium(III) with uncoordinated vinyl chain end.

this mechanism, in contrast to the case discussed above for Cr(II). The steady-state ethylene consumption rate (neglecting the contribution from ethylene consumption during the termination step) is given by eq 2 (see Supporting Information for derivation):

$$r_{C_2H_4} \approx k_{init} \frac{k_{\pi-insert}}{k_{\pi-insert} + k_{-init}} \frac{k_{insert}}{k_{H-Xfer}} K_{bind} P \qquad (2)$$

Using the computed free energies, the rate of ethylene uptake is 1×10^{-6} C_2H_4 site^{-1} s^{-1}, or 1×10^{-4} kg PE (mol Cr)$^{-1}$ h^{-1} at 373 K and 1 atm. Adjusting for the reported experimental conditions (343 K and 6 atm),[23] the computed rate is 6×10^{-7} C_2H_4 site^{-1} s^{-1}, or 6×10^{-5} kg PE (mol Cr)$^{-1}$ h^{-1}. The discrepancy is 6 orders of magnitude relative to the experimentally measured activity of 100 kg PE (mol Cr)$^{-1}$ h^{-1}. Results with B3LYP-D3 (Table S23) are similar. Furthermore, the total abundance of propagating sites (i.e, all sites with bridging hydroxyls) is extremely low (eq 3; see Supporting Information for derivation):

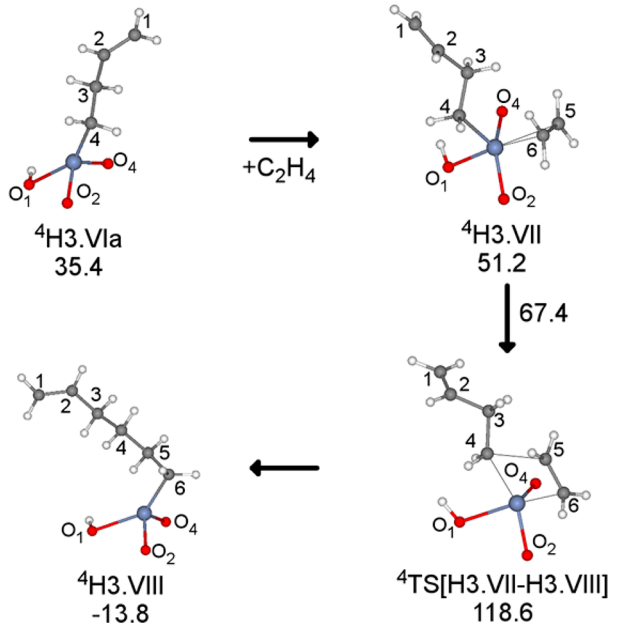

Figure 15. Stationary points for Cossee–Arlman propagation on a Cr(III) site, and free energies (kJ/mol) relative to that of the bare site, ^{4}**H3.I**, at 373 K. ^{4}**H3.VIa**, butenylchromium(III) with uncoordinated vinyl chain end; ^{4}**H3.VII**, (ethylene)(butenyl)chromium(III); ^{4}**TS**-[**H3.VII-H3.VIII**], transition state for insertion of coordinated ethylene into the Cr–C4 bond; ^{4}**H3.VIII**, hexenylchromium(III) with β-agostic interaction.

$$\tilde{\theta}_{prop} \approx \frac{k_i k_{\pi-insert}(1 + K_{bind}P)}{k_{H-Xfer}(k_{\pi-insert} + k_{reverse})} \qquad (3)$$

At 373 K and 1 atm, the predicted abundance is $10^{-7.3\pm4.1}$ (see Supporting Information for uncertainty estimation) and is even lower under the reported experimental conditions (343 K and 6 atm): $10^{-7.9\pm4.5}$. The vanishingly small predicted abundance is troubling because of the authors' claim[23] that the propagating sites are spectroscopically observable. Ascribing the 8-orders-of-magnitude discrepancy to DFT errors would invoke atypically large computational uncertainties, ~52 kJ/mol = k_BT ln[$10^{7.9}$] at temperatures typical of catalyst operation.[79]

Delley et al. did not consider coordination of ethylene prior to proton transfer (Figure 16, top path, ^{4}**H3.VII** → ^{4}**TS**-[**H3.VII-H3.IX**] → ^{4}**H3.IX**), which leads to a much faster termination pathway (geometries in Table S24). A lower energy pathway is expected in view of the ethylene-assisted pathway for initiation by proton transfer that is nearly its microscopic reverse (Figure 14, upper path). The transition state for ethylene-assisted termination, ^{4}**TS**[**H3.VII-H3.IX**], is lower in free energy than ^{4}**TS**[**H3.VIa-H3.Xa**] by 13 kJ/mol at 373 K. Under the conditions used in the previous computations (298 K), the difference is even larger, 26 kJ/mol. Furthermore, the free energy barrier to reach ^{4}**TS**[**H3.VII-H3.IX**], 70 kJ/mol ($k_{\pi,H\text{-}Xfer} = 1 \times 10^3$ site^{-1} s^{-1}), is nearly the same as the ethylene insertion barrier. Thus, only oligomers should form at this site,

DOI: 10.1021/acscatal.5b00016
ACS Catal. 2015, 5, 3360–3374

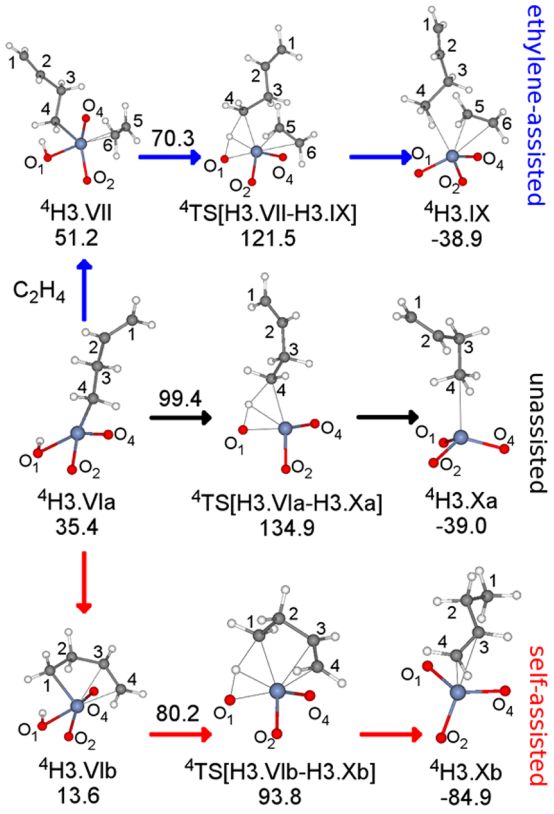

Figure 16. Stationary points for three possible termination pathways involving proton transfer over a Cr(III) site, and free energies (kJ/mol) relative to that of the bare site, ^{4}**H3.I**, at 373 K. Unassisted proton transfer (black): ^{4}**H3.VIa**, butenylchromium(III); ^{4}**TS**[**H3.VIa-H3.Xa**], transition state for direct proton transfer; ^{4}**H3.Xa**, 1-butene complex with methyl end near Cr. Ethylene-assisted proton transfer (blue): ^{4}**H3.VII**, (ethylene)(butenyl)chromium(III); ^{4}**TS**[**H3.VII-H3.IX**], transition state for proton transfer in ethylene complex; ^{4}**H3.IX**, (ethylene)(1-butene) complex with methyl end coordinated to Cr. Self-assisted proton transfer (red): ^{4}**H3.VIb**, butenylchromium(III) with coordinated vinyl chain end; ^{4}**TS**[**H3.VIb-H3.Xb**], transition state for direct proton transfer in complex with coordinated vinyl chain end; ^{4}**H3.Xb**, (1-butene)chromium(III).

instead of polymer chains. Increasing the ethylene pressure, which increases the rate of insertion, does not change this result and led to long polymer chains because ethylene-assisted reverse proton transfer becomes faster, as well.

The alkenyl ligand on Cr(III) can also play the role of the stabilizing olefin by coordinating to Cr through its vinyl end (Figure 16, lower path). Butenylchromium(III) with a coordinated vinyl chain end, ^{4}**H3.VIb** (Table S25), is 22 kJ/mol lower in free energy than ^{4}**H3.VIa** ($K_{\text{vinyl coord}} = 1 \times 10^3$), and 38 kJ/mol lower than the ethylene complex ^{4}**H3.VII**. The free energy barrier for proton transfer is 80 kJ/mol ($k_{\text{vinylH-Xfer}} = 5 \times 10$ site^{-1} s^{-1}), just slightly higher than the 70 kJ/mol for ethylene-assisted termination. However, the overall barrier to reach ^{4}**TS**[**H3.VIb-H3.Xb**] from ^{4}**H3.VIa** is 28 kJ/mol lower in free energy than the barrier for ethylene-assisted termination from the same point and 25 kJ/mol lower than the transition state for ethylene insertion. The resulting 1-butene complex, ^{4}**H3.Xb**, is considerably more stable than either ^{4}**H3.IX** or ^{4}**H3.X**. Subsequent coordination of ethylene must be followed by another highly unfavorable proton transfer to reactivate the site.

The problem of fast termination by self-assisted proton transfer could potentially be averted if the butenyl ligand undergoes β-H elimination instead (Figure 17). A hydride is

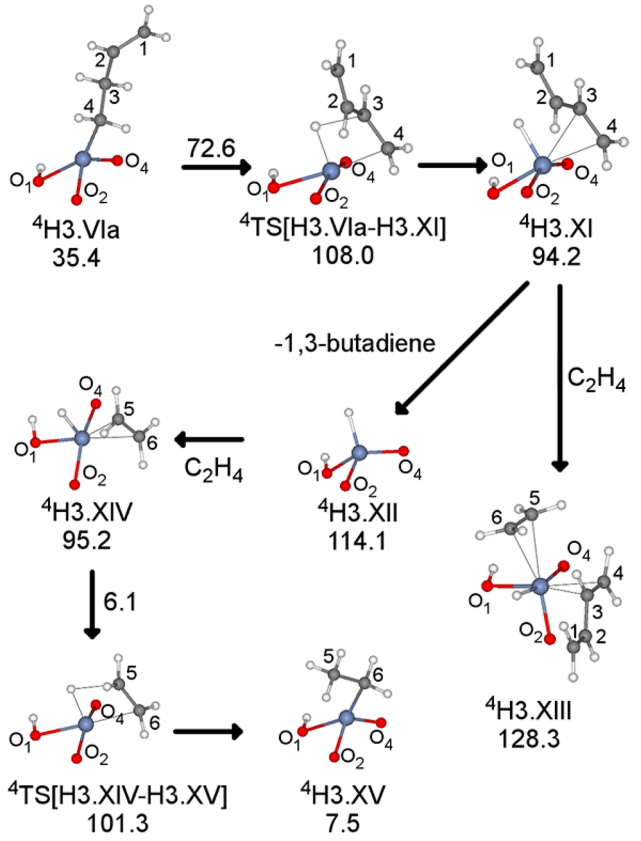

Figure 17. Stationary points for chain termination by β-H elimination over a Cr(III) site and free energies (kJ/mol) relative to that of the bare site, ^{4}**H3.I**, at 373 K. ^{4}**H3.VIa**, butenylchromium(III); ^{4}**TS**[**H3.VIa-H3.XI**], transition state for β-H elimination to Cr; ^{4}**H3.XI**, (1,3-butadiene)(hydrido)chromium(III); ^{4}**H3.XII**, hydridochromium(III); ^{4}**H3.XIII**, (ethylene)(1,3-butadiene)(hydrido)chromium(III); ^{4}**H3.XIV**, (ethylene)(hydrido)chromium(III); ^{4}**TS**[**H3.XIV-H3.XV**], transition state for ethylene insertion into the Cr−H bond; ^{4}**H3.XV**, ethylchromium(III).

transferred from C3 of the butenylchromium(III) site ^{4}**H3.VIa** to the metal, forming the coordinated 1,3-butadiene complex ^{4}**H3.XI** (Table S26). The free energy barrier for this reaction is 73 kJ/mol, and the transition state ^{4}**TS**[**H3.VIa-H3.XI**] is only 14 kJ/mol higher than that of vinyl-assisted proton transfer. The conjugation of 1,3-butadiene stabilizes the transition state because the free energy barrier for the analogous reaction of hexenylchromium(III) is higher, at 88 kJ/mol (Figure S3 and Table S27). At 373 K, 1,3-butadiene desorbs prior to ethylene binding (^{4}**H3.XIII**). The resulting hydridochromium(III) ^{4}**H3.XII** binds ethylene readily, followed by facile insertion to form the ethylchromium(III) complex ^{4}**H3.XV**.

Figure 18 summarizes the principal features of ethylene polymerization initiated by proton-transfer activation of the Cr(III) site. Our results suggest that this polymerization mechanism is not viable because, according to the single-site model considered here, too many sites are trapped in the dormant ^{4}**H3.III** state; a vanishingly small number escape to participate in the catalytic cycle.

DOI: 10.1021/acscatal.5b00016
ACS Catal. 2015, 5, 3360−3374

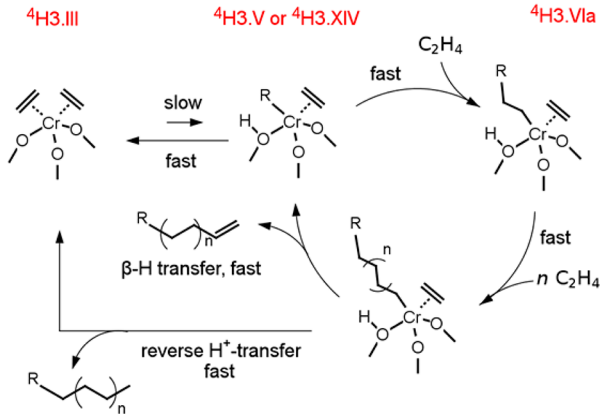

Figure 18. Principal features of a modified Phillips mechanism involving initiation by proton transfer, followed by repeated ethylene insertion at a Cr(III) active site and termination by reverse proton transfer (outer loop).[23] The need to reactivate the site after termination of each polymer chain makes the outer loop exceedingly slow. A potentially faster cycle would involve β-H termination (inner loop), which does not require reinitiation for every chain. However, the preferred reverse-H$^+$ transfer termination step traps the overwhelming majority of sites in the dormant ^{4}**H3.III** site.

3.7. Comparison of Proton-Transfer-Initiated Mechanisms at Cr(II) vs Cr(III) Sites. Conley et al.[22] reported that a model Cr(II)/SiO_2 catalyst is inactive for polymerization, whereas a model Cr(III)/SiO_2 catalyst is active, and proposed a proton transfer mechanism for the latter; however, comparison of the proton transfer-initiated pathways starting from Cr(II) and Cr(III) reveals that both oxidation states encounter the same issues (Figure 19). First, initiation is extremely slow. For Cr(III), the effective free energy barrier for proton transfer is 163 kJ/mol (**II** → **V**). For Cr(II), the barrier is slightly lower, 152 kJ/mol (**III** → **VIa**), although the highest transition state involves ethylene insertion into the Cr−vinyl bond following proton transfer. The free energy barriers for propagation are similar for both systems (**VIa** → **VIII**). From **VIa**, the ethylene insertion barrier is 83 kJ/mol for Cr(III). For Cr(II), the complex **VII** is slightly more stable than **VIa**, and the free energy barrier to insert ethylene is 86 kJ/mol. However, the most stable species prior to insertion is actually the vinyl-coordinated species **VIb**. The effective free energies to reach the transition state **TS**[**VII**−**VIII**] are 109 and 105 kJ/mol for Cr(II) and Cr(III), respectively. Finally, the most favorable termination step, self-assisted proton transfer (**VIb** → **Xb**), involves barriers of 45 and 80 kJ/mol for Cr(II) and Cr(III), respectively. Oligomers, not polymers, are expected to form in both cases. Our calculations suggest that the difference in oxidation states does not change the infeasibility of the proton-transfer initiated mechanism.

3.8. Cossee−Arlman Chain Growth at a Monoalkylchromium(III) Site (CA). Ethylene insertion into the metal−carbon bond of a monoalkylchromium(III) species has long been considered the most likely propagation mechanism for the Phillips catalyst,[1,7,13] despite continuing uncertainty over how it might initially be formed. The starting structure for this Cossee−Arlman mechanism, the *n*-butylchromium(III) site ^{4}**CA.I** shown in Figure 20, was optimized in its high-spin, quartet ground state. It is the reference free energy state for all subsequent structures in this mechanism. Ethylene binds with Cr−C distances of 2.48 and 2.61 Å (^{4}**CA.II**, Table S28). Relative to ^{4}**CA.I**, our calculated binding energy of −52 kJ/mol differs from the −35 kJ/mol calculated by Espelid and Børve.[13] However, both we and they find that this modest binding energy does not offset the entropy penalty for immobilizing free ethylene: we find an overall free

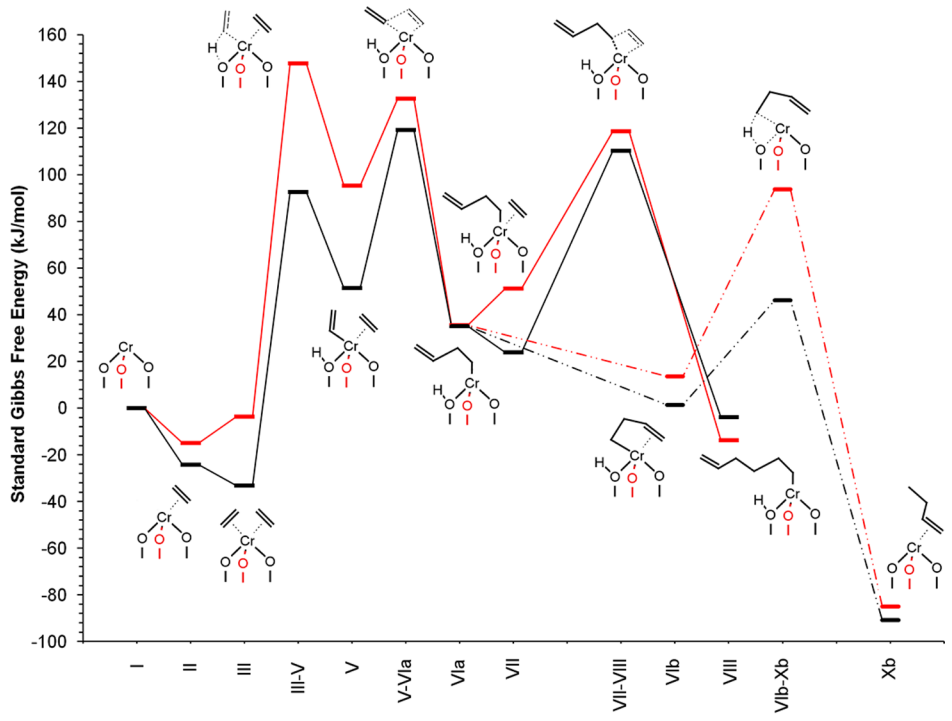

Figure 19. Comparison of proton-transfer-initiated alkylation (solid lines), subsequent Cossee−Arlman insertion (solid lines), and chain termination (dashed lines) for Cr(II) (black) and Cr(III) (red) precursors. Results computed with ωB97X-D at 373 K and 1 atm.

DOI: 10.1021/acscatal.5b00016
ACS Catal. 2015, 5, 3360−3374

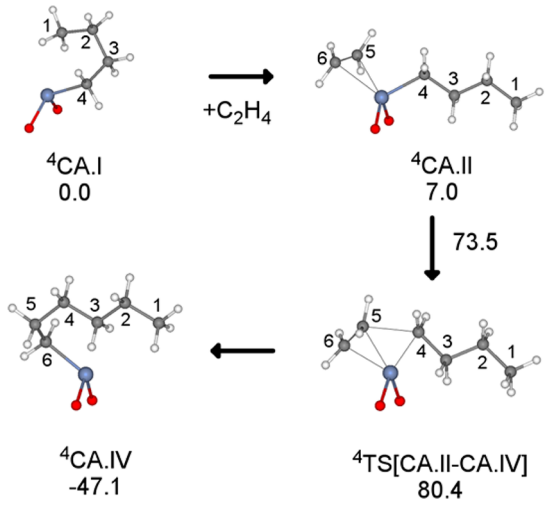

Figure 20. Stationary points for Cossee−Arlman propagation on a monoalkylchromium(III) site represented by *n*-butylchromium(III), **^{4}CA.I**, and free energies (kJ/mol) relative to that site, at 373 K. **^{4}CA.II**, (ethylene)(*n*-butyl)chromium; **^{4}TS[CA.II-CA.IV]**, transition state for insertion of coordinated ethylene into the Cr−C4 bond; **^{4}CA.IV**, *n*-hexylchromium.

energy change of +7 kJ/mol at 373 K and 1 atm, corresponding to a binding constant K of 0.11 atm^{-1}.

As the coordinated monomer prepares to insert, the Cr−C4 bond begins to stretch in the transition state **^{4}TS[CA.II-CA.IV]**. At the same time, a new bond forms as the distance between C4 and C5 shrinks from 3.15 to 2.14 Å. These values match those reported by Espelid and Børve (Table S28). The overall free energy barrier to traverse the saddle point, 73 kJ/mol relative to **^{4}CA.II**, is low enough for fast propagation, with a calculated rate constant k_{prop} = 4 × 10^2 s^{-1} site^{-1} at 373 K. The activation energy relative to **^{4}CA.II** (64 kJ/mol) also agrees with the value reported by Espelid and Børve (56 kJ/mol).

Chain termination by β-H elimination is shown in Figure 21. Migration of a β-H from the alkyl ligand to Cr gives **^{4}CA.III**. In the transition state, **^{4}TS[CA.I-CA.III]**, the β-H approaches Cr at a distance of 1.61 Å. The Cr−C4 bond is weakened (Table S29) as a π-bond begins to develop between C3 and C4. The free energy of the transition state relative to **^{4}CA.I**, 81 kJ/mol, is essentially the same as the barrier for propagation (80 kJ/mol).

The active site is regenerated when 1-butene desorbs from **^{4}CA.III**. The resulting metal hydride intermediate, **^{4}CA.V**, is uphill by 20 kJ/mol relative to **^{4}CA.III**. However, our calculation assumes that 1-butene (representing the polymer product) is present at the standard state pressure of 1 atm. Under realistic operating conditions, the product is present at a much lower pressure than ethylene and will desorb readily. In addition, because higher α-olefins and long polymer chains gain much more translational entropy from desorption compared to 1-butene, all subsequent species in the reaction pathway should be lower in energy.

After ethylene binds to form **^{4}CA.VI**, the transition state for the next ethylene insertion, **^{4}TS[CA.VI-CA.VII]**, has a calculated free energy of 81 kJ/mol relative to **^{4}CA.I**. This is indistinguishable from the barrier for β-H elimination. However, the computed free energy of **^{4}TS[CA.VI-CA.VII]** is likely too high as a result of the underestimated desorption

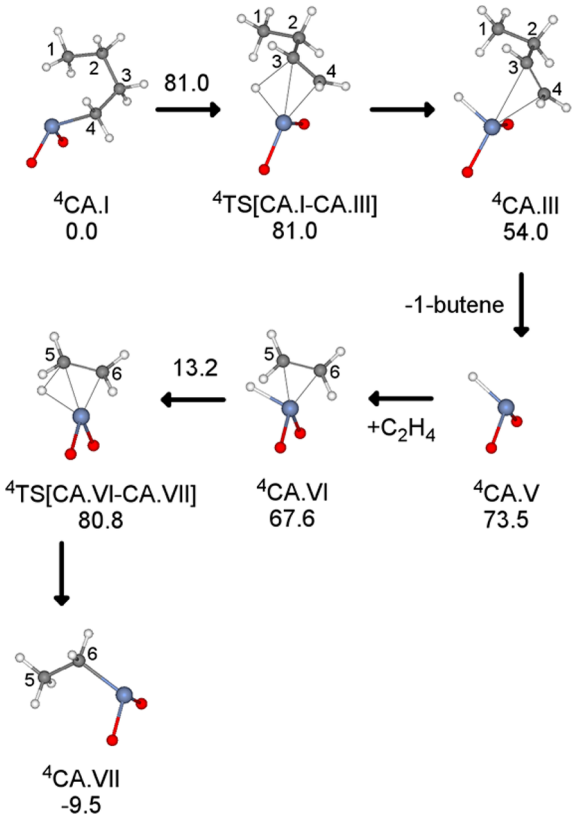

Figure 21. Stationary points for chain termination by β-H elimination and subsequent ethylene insertion into the resulting Cr−H bond at 373 K. **^{4}CA.I**, *n*-butylchromium(III); **^{4}TS[CA.I-CA.III]**, transition state for β-H transfer to Cr; **^{4}CA.III**, (1-butene)(hydrido)chromium-(III); **^{4}CA.V**, hydridochromium(III); **^{4}CA.VI**, (ethylene)(hydrido)-chromium(III); **^{4}TS[CA.VI-CA.VII]**, transition state for ethylene insertion into the Cr−H bond; **^{4}CA.VII**, ethylchromium(III).

free energy of the polymer chain (represented by 1-butene) in the previous step. Therefore, the earlier transition state **^{4}TS-[CA.I-CA.III]** is probably the main hurdle for the overall chain termination/regeneration process. Overall, the calculated rate coefficient, k_{elim}, for the reaction **^{4}CA.I** → **^{4}CA.III** is 36 s^{-1} site^{-1}.

An alternative chain termination reaction is β-H transfer to the monomer, in which the bound ethylene in **^{4}CA.II** becomes an ethyl ligand and so transforms the existing alkyl ligand into a bound α-olefin (Figure 22). The transition state **^{4}TS[CA.II-CA.IX]** (Table S30) is 99 kJ/mol higher in free energy than **^{4}CA.II**, corresponding to a rate constant k_{xfer} = 0.1 s^{-1} site^{-1} at 373 K. This transition state is also 25 kJ/mol higher in free energy than the β-H elimination transition state **^{4}TS[CA.I-CA.III]**. However, the rate of β-H transfer to monomer increases with ethylene pressure, but that of β-H elimination does not.

A microkinetic model can be constructed from these DFT results. The steady-state ethylene uptake rate is primarily due to the rate of ethylene insertion into a Cr−C bond:

$$r_{C_2H_4} = k_{prop}\frac{K_1P}{1 + K_1P} \quad (4)$$

At 373 K and 40 atm, the computed ethylene uptake rate is $10^{2.5\pm2.8}$ C_2H_4 s^{-1} site^{-1} (see Supporting Information S.5 for uncertainty estimation, including a CCSD(T) test of the model chemistry), which is similar to an experimental value of 2 × 10^3

DOI: 10.1021/acscatal.5b00016
ACS Catal. 2015, 5, 3360−3374

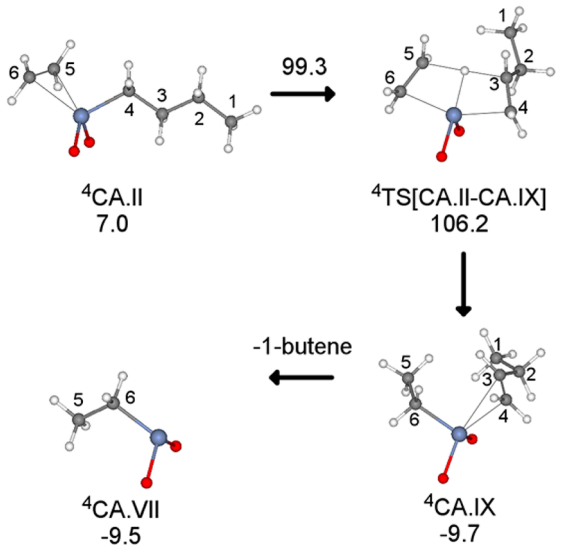

Figure 22. Stationary points for β-H transfer to monomer, and free energies (kJ/mol) relative to *n*-butylchromium(III) ^{4}**CA.I** at 373 K. ^{4}**CA.II**, *n*-butylchromium; ^{4}**CA.IX**, (ethylene)(*n*-butyl)chromium; ^{4}**TS**[**CA.II-CA.IX**], transition state for β-H transfer to C5; ^{4}**CA.IX**, (1-butene)ethylchromium; ^{4}**CA.VII**, ethylchromium.

C_2H_4 s^{-1} Cr^{-1} measured for these conditions at low Cr loading (0.01 wt % Cr).[2] Because β-H transfer to monomer contributes only 0.02% of the rate (see Supporting Information for full derivation), a large kinetic isotope effect is not expected for this mechanism. A range for the experimental apparent free energy barriers was also estimated using eq 4, assuming an activity of 2 × 10^3 C_2H_4 s^{-1} Cr^{-1} at 373 K and 40 atm. Because the Langmuir term is neither first- nor zeroth-order in ethylene pressure under these conditions, barriers were computed at the low and high pressure limits, according to eqs 5 and 6, respectively:

$$\Delta G^{\ddagger}_{app} = k_B T \ln\left[\frac{h}{k_B T} k_{prop}\right] \quad (5)$$

$$\Delta G^{\ddagger}_{app} = k_B T \ln\left[\frac{h}{k_B T} k_{prop} K_1 \frac{P_0}{P}\right] \quad (6)$$

The resulting barriers are 68 and 80 kJ/mol, respectively.

The weight-averaged molecular weight of the polyethylene is determined by the ratio of propagation and termination rates,[80,81] eq 7 (see Supporting Information for full derivation):

$$M_w = 2\frac{k_{xfer}K_1P + 2k_{prop}K_1P + k_{elim}}{k_{xfer}K_1P + k_{elim}} \quad (7)$$

At 373 K and for pressures in the range 1−40 atm, predicted M_w values range from 100 to 3000 g/mol, which are smaller than the 10^4−10^6 g/mol values reported for the Phillips catalyst,[1,82,83] but still reasonable given the typical DFT errors. As observed experimentally, the molecular weight is predicted to level off at ∼2 × 10^5 g/mol, according to eq 8:

$$M_{w,high P} = 2\frac{k_{xfer} + 2k_{prop}}{k_{xfer}} \quad (8)$$

However, this occurs at pressures of ∼10^4 atm, compared with 10^2 atm required experimentally.[84] We attribute the difference to small errors in the DFT calculations, which can have effects of this magnitude on predicted rate and binding coefficients and molecular weights. In addition, small changes in the site geometry may alter the rate coefficients and equilibrium constants of the elementary steps.[44,85]

4. CONCLUSIONS

The calculated free energy barriers for initiation, propagation, and termination for each mechanism in this study are summarized in Table 2. Starting from the Cr(II) site investigated here, the free energy barriers for propagation in the metallacycle and Green−Rooney mechanisms are much too high to account for the observed polymerization rates, in agreement with earlier conclusions.[13,17,18] The oxachromacycle mechanism has an appropriately low propagation barrier of 97 kJ/mol, but initiation is far too slow, with a free energy barrier of 165 kJ/mol. Initiation of a Cossee−Arlman mechanism by proton transfer to create a bridging hydroxyl is similarly much too slow for both Cr(II) and Cr(III) sites, and termination is much too fast: only short oligomers would form.

Thus far, Cossee−Arlman propagation at a monoalkylchromium(III) site *without an adjacent bridging hydroxyl* or *vinyl end* is the only viable mechanism we (or others) have identified, although the reactions that lead to its initial formation remain unknown. In this model, termination also occurs, but the resulting site remains active with no need

Table 2. Summary of Free Energy Barriers (kJ/mol) for Various Proposed Phillips Mechanisms at T = 373 K and P = 1 atm

mechanism, propagating site	$\Delta G^{\ddagger}_{init}$	$\Delta G^{\ddagger}_{prop}$	$\Delta G^{\ddagger}_{term}$	$\Delta G^{\ddagger}_{app}$ [a]	comments
(M) metallacycle, (≡SiO)$_2$Cr^{IV}[*c*-(CH$_2$)$_n$]		149−189	114		(1) $\Delta G^{\ddagger}_{prop}$ too high (2) $\Delta G^{\ddagger}_{prop} > \Delta G^{\ddagger}_{term}$
(O) oxachromacycle, (≡SiO)$_2$Cr^{II}[*c*-(CH$_2$)$_n$]	165	97			$\Delta G^{\ddagger}_{init}$ too high
(C) Green−Rooney, (≡SiO)$_2$Cr^{IV}=CHR		226			$\Delta G^{\ddagger}_{prop}$ too high
Cossee−Arlman Mechanisms					
(H2) (≡SiO)Si(OH)Cr^{II}R	152	109	45	216	(1) $\Delta G^{\ddagger}_{init}$ high and reinitiation required (2) $\Delta G^{\ddagger}_{prop} > \Delta G^{\ddagger}_{term}$ (oligomers only)
(H3) (≡SiO)$_2$Si(OH)Cr^{III}R	163	105	80	187	(1) $\Delta G^{\ddagger}_{init}$ high and reinitiation required (2) makes oligomers even at high pressure
(CA) (≡SiO)$_2$Cr^{III}R		79	80	79	(1) termination creates new active site (2) unknown initiation
experimental values[2]				68−80	

[a]For the H2 and H3 mechanisms, $\Delta G^{\ddagger}_{app} = \Delta G^{\ddagger}_{init} + \Delta G^{\ddagger}_{prop} - \Delta G^{\ddagger}_{term}$. For the CA mechanism, $\Delta G^{\ddagger}_{app} \approx \Delta G^{\ddagger}_{prop}$.

DOI: 10.1021/acscatal.5b00016
ACS Catal. 2015, 5, 3360−3374

for reinitiation, as required by McDaniel's postulates,[9] and long polymer chains are formed at elevated pressures.

Because the Phillips catalyst is usually made with an amorphous silica, the origin of the high polyethylene dispersity is plausibly ascribed to a large number of distinct active sites. Thus, it is reasonable that a single-site model will not be capable of modeling all aspects of Phillips polymerization. Recently, Goldsmith et al.[85,86] showed how subtle structural variations in sites present on amorphous SiO_2 can lead to substantial changes in reactivity and, by extension, to changes in the degree of polymerization. However, Goldsmith et al. found that the propagation steps in the Cossee−Arlman mechanism are only mildly sensitive to to the local site structure.[86] Nevertheless, predictions for mechanisms that invoke changes in the bonds between Cr and support atoms may depend strongly on the local active site structure. These mechanisms include the oxachromacycle propagation mechanism introduced in this work as well as previously proposed initiation mechanisms involving rare silanols.[17,87]

■ ASSOCIATED CONTENT

Supporting Information

The following file is available free of charge on the ACS Publications website at DOI: 10.1021/acscatal.5b00016.

Bonds, angles, imaginary frequencies, Cartesian coordinates, absolute energies, number of imaginary frequencies, spin contamination (PDF)

■ AUTHOR INFORMATION

Corresponding Authors

*Phone: +1 805 893-5606. Fax: +1 805 893 4731. E-mail: sscott@engineering.ucsb.edu.

*Phone: +1 805 284-8293. Fax: +1 805 893 4731. E-mail: baronp@engineering.ucsb.edu.

Notes

The authors declare no competing financial interest.

■ ACKNOWLEDGMENTS

This work was supported by the U.S. Department of Energy, Office of Science, Office of Basic Energy Sciences, under the Catalysis Science Initiative (DE-FG-02-03ER15467) and the National Science Foundation, Award no. CBET08-54425. We thank Horia Metiu for helpful discussions.

■ REFERENCES

(1) McDaniel, M. P. *Adv. Catal.* **2010**, *53*, 123−606.

(2) Leach, B. E. *Applied Industrial Catalysis*. Academic Press: New York, 1983.

(3) McDaniel, M. P.; Welch, M. B. *J. Catal.* **1983**, *82*, 98−109.

(4) McDaniel, M. P. *Adv. Catal.* **1985**, *33*, 47−98.

(5) McDaniel, M. P.; Welch, M. B.; Dreiling, M. J. *J. Catal.* **1983**, *82*, 118−126.

(6) Pullukat, T. J.; Hoff, R. E.; Shida, M. *J. Polym. Sci., Polym. Chem. Ed.* **1980**, *18*, 2857−2866.

(7) Hogan, J. P. *J. Polym. Sci., Part A-1: Polym. Chem.* **1970**, *8*, 2637−2652.

(8) Cossee, P. *J. Catal.* **1964**, *3*, 80−88.

(9) McDaniel, M. P. Review of the Phillips Chromium Catalyst for Ethylene Polymerization. In *Handbook of Heterogeneous Catalysis*; Wiley-VCH: Weinheim, 2008; pp 3733−3792.

(10) Groppo, E.; Lamberti, C.; Bordiga, S.; Spoto, G.; Zecchina, A. *Chem. Rev.* **2005**, *105*, 115−183.

(11) McGuinness, D. S.; Davies, N. W.; Horne, J.; Ivanov, I. *Organometallics* **2010**, *29*, 6111−6116.

(12) Cheng, R. H.; Xu, C.; Liu, Z.; Dong, Q.; He, X. L.; Fang, Y. W.; Terano, M.; Hu, Y. T.; Pullukat, T. J.; Liu, B. P. *J. Catal.* **2010**, *273*, 103−115.

(13) Espelid, O.; Børve, K. J. *J. Catal.* **2000**, *195*, 125−139.

(14) McDaniel, M. P.; Cantor, D. M. *J. Polym. Sci., Polym. Chem. Ed.* **1983**, *21*, 1217−1221.

(15) Ghiotti, G.; Garrone, E.; Zecchina, A. *J. Mol. Catal.* **1988**, *46*, 61−77.

(16) Kantcheva, M.; Dallalana, I. G.; Szymura, J. A. *J. Catal.* **1995**, *154*, 329−334.

(17) Schmid, R.; Ziegler, T. *Can. J. Chem.* **2000**, *78*, 265−269.

(18) Zhong, L.; Liu, Z.; Cheng, R. H.; Tang, S. Y.; Qiu, P. Y.; He, X. L.; Terano, M.; Liu, B. P. *ChemCatChem* **2012**, *4*, 872−881.

(19) Kuran, W. *Principles of Coordination Polymerisation*; Wiley: Chichester; New York, 2001, p 93.

(20) Merryfield, R.; McDaniel, M.; Parks, G. *J. Catal.* **1982**, *77*, 348−359.

(21) Zecchina, A.; Groppo, E. *Proc. R. Soc. London, Ser. A* **2012**, *468*, 2087−2098.

(22) Conley, M. P.; Delley, M. F.; Siddiqi, G.; Lapadula, G.; Norsic, S.; Monteil, V.; Safonova, O. V.; Copéret, C. *Angew. Chem., Int. Ed.* **2014**, *53*, 1872−1876.

(23) Delley, M. F.; Nũnez-Zarur, F.; Conley, M. P.; Comas-Vives, A.; Siddiqi, G.; Norsic, S.; Monteil, V.; Safonova, O. V.; Copéret, C. *Proc. Natl. Acad. Sci. U. S. A.* **2014**, *111*, 11624−11629.

(24) Huenerbein, R.; Schirmer, B.; Moellmann, J.; Grimme, S. *Phys. Chem. Chem. Phys.* **2010**, *12*, 6940−6948.

(25) Siegbahn, P. E. M. *Faraday Discuss.* **2003**, *124*, 289−296.

(26) Frisch, M. J.; Trucks, G. W.; Schlegel, H. B.; Scuseria, G. E.; Robb, M. A.; Cheeseman, J. R.; Scalmani, G.; Barone, V.; Mennucci, B.; Petersson, G. A.; Nakatsuji, H.; Caricato, M.; Li, X.; Hratchian, H. P.; Izmaylov, A. F.; Bloino, J.; Zheng, G.; Sonnenberg, J. L.; Hada, M.; Ehara, M.; Toyota, K.; Fukuda, R.; Hasegawa, J.; Ishida, M.; Nakajima, T.; Honda, Y.; Kitao, O.; Nakai, H.; Vreven, T.; Montgomery, J. A.; Peralta, J. E.; Ogliaro, F.; Bearpark, M.; Heyd, J. J.; Brothers, E.; Kudin, K. N.; Staroverov, V. N.; Kobayashi, R.; Normand, J.; Raghavachari, K.; Rendell, A.; Burant, J. C.; Iyengar, S. S.; Tomasi, J.; Cossi, M.; Rega, N.; Millam, J. M.; Klene, M.; Knox, J. E.; Cross, J. B.; Bakken, V.; Adamo, C.; Jaramillo, J.; Gomperts, R.; Stratmann, R. E.; Yazyev, O.; Austin, A. J.; Cammi, R.; Pomelli, C.; Ochterski, J. W.; Martin, R. L.; Morokuma, K.; Zakrzewski, V. G.; Voth, G. A.; Salvador, P.; Dannenberg, J. J.; Dapprich, S.; Daniels, A. D.; Farkas, Ö.; Foresman, J. B.; Ortiz, J. V.; Cioslowski, J.; Fox, D. J. *Gaussian 09, Revision A.1*; Gaussian, Inc.: Wallingford CT, 2009.

(27) Chai, J. D.; Head-Gordon, M. *Phys. Chem. Chem. Phys.* **2008**, *10*, 6615−6620.

(28) Goerigk, L.; Grimme, S. *Phys. Chem. Chem. Phys.* **2011**, *13*, 6670−6688.

(29) Schenker, S.; Schneider, C.; Tsogoeva, S. B.; Clark, T. *J. Chem. Theory Comput.* **2011**, *7*, 3586−3595.

(30) Zhao, Y.; Truhlar, D. G. *J. Chem. Theory Comput.* **2011**, *7*, 669−676.

(31) Yang, K.; Zheng, J. J.; Zhao, Y.; Truhlar, D. G. *J. Chem. Phys.* **2010**, *132*, 164117.

(32) Minenkov, Y.; Singstad, A.; Occhipinti, G.; Jensen, V. R. *Dalton Trans.* **2012**, *41*, 5526−5541.

(33) Feller, D. *J. Comput. Chem.* **1996**, *17*, 1571−1586.

(34) Schuchardt, K. L.; Didier, B. T.; Elsethagen, T.; Sun, L. S.; Gurumoorthi, V.; Chase, J.; Li, J.; Windus, T. L. *J. Chem. Inf. Model.* **2007**, *47*, 1045−1052.

(35) Godbout, N.; Salahub, D. R.; Andzelm, J.; Wimmer, E. *Can. J. Chem.* **1992**, *70*, 560−571.

(36) Schlegel, H. B. *J. Comput. Chem.* **1982**, *3*, 214−218.

(37) Baker, J. *J. Comput. Chem.* **1986**, *7*, 385−395.

(38) Jensen, F. *Introduction to Computational Chemistry*; Wiley: Chichester, New York, 1999.

DOI: 10.1021/acscatal.5b00016
ACS Catal. 2015, 5, 3360−3374

(39) McDaniel, M. P.; Rohlfing, D. C.; Benham, E. A. *Polym. React. Eng.* **2003**, *11*, 101−132.
(40) Weckhuysen, B. M.; Schoonheydt, R. A. *Catal. Today* **1999**, *51*, 215−221.
(41) Thüne, P. C.; Loos, J.; Chen, X. H.; van Kimmenade, E. M. E.; Kong, B.; Niemantsverdriet, J. W. H. *Top. Catal.* **2007**, *46*, 239−245.
(42) Waddell, W. H.; Evans, L. R. Silica, Amorphous Silica. In *Kirk-Othmer Encyclopedia of Chemical Technology*; Wiley: Chichester, New York, 2000.
(43) Gaskell, P. H.; Parker, J. M.; Davis, E. A. *The Structure of Non-Crystalline Materials*; Taylor & Francis: New York, NY, 1983.
(44) Demmelmaier, C. A.; White, R. E.; van Bokhoven, J. A.; Scott, S. L. *J. Catal.* **2009**, *262*, 44−56.
(45) Delley, M. F.; Conley, M. P.; Copéret, C. *Catal. Lett.* **2014**, *144*, 805−808.
(46) Lee, C. T.; Yang, W. T.; Parr, R. G. *Phys. Rev. B: Condens. Matter Mater. Phys.* **1988**, *37*, 785−789.
(47) Becke, A. D. *J. Chem. Phys.* **1993**, *98*, 5648−5652.
(48) Hay, P. J.; Wadt, W. R. *J. Chem. Phys.* **1985**, *82*, 299−310.
(49) Hay, P. J.; Wadt, W. R. *J. Chem. Phys.* **1985**, *82*, 270−283.
(50) Wadt, W. R.; Hay, P. J. *J. Chem. Phys.* **1985**, *82*, 284−298.
(51) Mclean, A. D.; Chandler, G. S. *J. Chem. Phys.* **1980**, *72*, 5639−5648.
(52) Krishnan, R.; Binkley, J. S.; Seeger, R.; Pople, J. A. *J. Chem. Phys.* **1980**, *72*, 650−654.
(53) Ehlers, A. W.; Bohme, M.; Dapprich, S.; Gobbi, A.; Hollwarth, A.; Jonas, V.; Kohler, K. F.; Stegmann, R.; Veldkamp, A.; Frenking, G. *Chem. Phys. Lett.* **1993**, *208*, 111−114.
(54) Roy, L. E.; Hay, P. J.; Martin, R. L. *J. Chem. Theory Comput.* **2008**, *4*, 1029−1031.
(55) Clark, T.; Chandrasekhar, J.; Spitznagel, G. W.; Schleyer, P. V. *J. Comput. Chem.* **1983**, *4*, 294−301.
(56) Grimme, S.; Ehrlich, S.; Goerigk, L. *J. Comput. Chem.* **2011**, *32*, 1456−1465.
(57) Grimme, S.; Antony, J.; Ehrlich, S.; Krieg, H. *J. Chem. Phys.* **2010**, *132*, 154104.
(58) Liu, Z.; Zhong, L.; Yang, Y.; Cheng, R. H.; Liu, B. P. *J. Phys. Chem. A* **2011**, *115*, 8131−8141.
(59) Perdew, J. P. *Phys. Rev. B: Condens. Matter Mater. Phys.* **1986**, *33*, 8822−8824.
(60) Vosko, S. H.; Wilk, L.; Nusair, M. *Can. J. Phys.* **1980**, *58*, 1200−1211.
(61) Cheng, R. H.; Liu, Z.; Qiu, P. Y.; Zhang, S. L.; Liu, B. P. *Chin. J. Polym. Sci.* **2008**, *26*, 579−587.
(62) Dixon, J. T.; Green, M. J.; Hess, F. M.; Morgan, D. H. *J. Organomet. Chem.* **2004**, *689*, 3641−3668.
(63) McGuinness, D. S. *Chem. Rev.* **2011**, *111*, 2321−2341.
(64) Ghiotti, G.; Garrone, E.; Zecchina, A. *J. Mol. Catal.* **1991**, *65*, 73−83.
(65) Groppo, E.; Lamberti, C.; Bordiga, S.; Spoto, G.; Zecchina, A. *J. Catal.* **2006**, *240*, 172−181.
(66) Nait Ajjou, J. A.; Scott, S. L.; Paquet, V. *J. Am. Chem. Soc.* **1998**, *120*, 415−416.
(67) Ruddick, V. J.; Badyal, J. P. S. *J. Phys. Chem. B* **1998**, *102*, 2991−2994.
(68) van Rensburg, W. J.; Grove, C.; Steynberg, J. P.; Stark, K. B.; Huyser, J. J.; Steynberg, P. J. *Organometallics* **2004**, *23*, 1207−1222.
(69) Yang, Y.; Liu, Z.; Cheng, R. H.; He, X. L.; Liu, B. P. *Organometallics* **2014**, *33*, 2599−2607.
(70) Baker, L. M.; Carrick, W. L. *J. Org. Chem.* **1970**, *35*, 774−776.
(71) Ivin, K. J.; Rooney, J. J.; Stewart, C. D.; Green, M. L. H.; Mahtab, R. *J. Chem. Soc., Chem. Commun.* **1978**, 604−606.
(72) Turner, H. W.; Schrock, R. R. *J. Am. Chem. Soc.* **1982**, *104*, 2331−2333.
(73) Turner, H. W.; Schrock, R. R.; Fellmann, J. D.; Holmes, S. J. *J. Am. Chem. Soc.* **1983**, *105*, 4942−4950.
(74) Fang, Y.; Liu, B.; Terano, M. *Kinet. Catal.* **2006**, *47*, 295−302.
(75) Liu, B. P.; Nakatani, H.; Terano, M. *J. Mol. Catal. A: Chem.* **2003**, *201*, 189−197.
(76) Nait Ajjou, J. A.; Scott, S. L. *J. Am. Chem. Soc.* **2000**, *122*, 8968−8976.
(77) Van Santen, R. A.; Kramer, G. J. *Chem. Rev.* **1995**, *95*, 637−660.
(78) Theopold, K. H. *Eur. J. Inorg. Chem.* **1998**, 15−24.
(79) Harvey, J. N. *Annu. Rep. Prog. Chem., Sect. C: Phys. Chem.* **2006**, *102*, 203−226.
(80) Keii, T. *Heterogeneous Kinetics: Theory of Ziegler−Natta−Kaminsky Polymerization*; Springer: New York, 2004.
(81) Tonosaki, K.; Taniike, T.; Terano, M. *J. Mol. Catal. A: Chem.* **2011**, *340*, 33−38.
(82) Kim, C. S.; Woo, S. I.; Jeong, D. J.; Oh, J. S. *Polym. Bull. (Heidelberg, Ger.)* **1992**, *29*, 205−212.
(83) Kissin, Y. V.; Brandolini, A. J.; Garlick, J. L. *J. Polym. Sci., Part A: Polym. Chem.* **2008**, *46*, 5315−5329.
(84) Clark, A.; Bailey, G. C. *J. Catal.* **1963**, *2*, 241−247.
(85) Goldsmith, B. R.; Sanderson, E. D.; Bean, D.; Peters, B. *J. Chem. Phys.* **2013**, *138*, 204105.
(86) Goldsmith, B. R.; Fong, A.; Peters, B. Understanding Reactivity with Reduced Potential Energy Landscapes: Recent Advances and New Directions. In *Reaction Rate Constant Computations: Theories and Applications*; Royal Society of Chemistry: Cambridge, UK, 2013; pp 213−232.
(87) Espelid, O.; Børve, K. J. *J. Catal.* **2002**, *205*, 366−374.

DOI: 10.1021/acscatal.5b00016
ACS Catal. 2015, 5, 3360−3374